WILEY

RESEARCH ARTICLE

Brain network dynamics in schizophrenia: Reduced dynamism of the default mode network

Akhil Kottaram[1] | Leigh A. Johnston[1,2] | Luca Cocchi[3] | Eleni P. Ganella[4,5,6] |
Ian Everall[5,7,8,9] | Christos Pantelis[4,5,6,9,10,11] | Ramamohanarao Kotagiri[12] |
Andrew Zalesky[1,4]

[1]Department of Biomedical Engineering, The University of Melbourne, Victoria, Australia

[2]Melbourne Brain Centre Imaging Unit, The University of Melbourne, Victoria, Australia

[3]Clinical Brain Networks Group, QIMR Berghofer Medical Research Institute, Brisbane, Queensland, Australia

[4]Melbourne Neuropsychiatry Centre, The University of Melbourne, Victoria, Australia

[5]Department of Psychiatry, The University of Melbourne, Victoria, Australia

[6]Schizophrenia Research Group, Cooperative Research Centre for Mental Health, Carlton, Victoria, Australia

[7]Psychology and Neuroscience, Institute of Psychiatry, Kings College London, London, United Kingdom

[8]South London and Maudsley NHS Foundation Trust, Bethlem Royal Hospital, Beckenham, United Kingdom

[9]Florey Institute for Neurosciences and Mental Health, Parkville, Victoria, Australia

[10]Department of Electrical and Electronic Engineering, Centre for Neural Engineering, The University of Melbourne, Victoria, Australia

[11]North Western Mental Health, Melbourne Health, Victoria, Australia

[12]Department of Computing and Information Systems, The University of Melbourne, Victoria, Australia

Correspondence
Akhil Kottaram, Department of Biomedical Engineering, Level 1, Building 261, 203 Bouverie Street, The University of Melbourne, Victoria 3010, Australia.
Email: akarazhma@student.unimelb.edu.au

Abstract

Complex human behavior emerges from dynamic patterns of neural activity that transiently synchronize between distributed brain networks. This study aims to model the dynamics of neural activity in individuals with schizophrenia and to investigate whether the attributes of these dynamics associate with the disorder's behavioral and cognitive deficits. A hidden Markov model (HMM) was inferred from resting-state functional magnetic resonance imaging (fMRI) data that was temporally concatenated across individuals with schizophrenia ($n = 41$) and healthy comparison individuals ($n = 41$). Under the HMM, fluctuations in fMRI activity within 14 canonical resting-state networks were described using a repertoire of 12 brain states. The proportion of time spent in each state and the mean length of visits to each state were compared between groups, and canonical correlation analysis was used to test for associations between these state descriptors and symptom severity. Individuals with schizophrenia activated default mode and executive networks for a significantly shorter proportion of the 8-min acquisition than healthy comparison individuals. While the default mode was activated less frequently in schizophrenia, the duration of each activation was on average 4–5 s longer than the comparison group. Severity of positive symptoms was associated with a longer proportion of time spent in states characterized by inactive default mode and executive networks, together with heightened activity in sensory networks. Furthermore, classifiers trained on the state descriptors predicted individual diagnostic status with an accuracy of 76–85%.

KEYWORDS

default mode network, hidden Markov model, neural dynamics, resting state fMRI, resting state networks, schizophrenia

1 | INTRODUCTION

Resting-state functional neuroimaging is widely used to investigate cerebral processes underlying the neurocognitive and behavioral deficits associated with schizophrenia. Most studies have employed functional magnetic resonance imaging (fMRI) or encephalographic modalities to derive *time-averaged* measures of regional activation and functional connectivity, which provide a summary of activity over the duration of the entire scan acquisition (Alexander-Bloch et al., 2010; Calhoun, Eichele, & Pearlson, 2009; Cocchi, Halford et al., 2014; Fornito, Yoon, Zalesky, Bullmore, & Carter, 2011; Fornito, Zalesky, Pantelis, & Bullmore, 2012; Gur & Gur, 2010; Kircher & Thienel, 2005; Liu et al., 2008; Rubinov et al., 2009; van den Heuvel & Fornito, 2014). However, these neuroimaging modalities yield data that is inherently *time-resolved*, and thus enable investigation of dynamics in neural activity and connectivity as a function of time.

Neural dynamics give rise to spatially distributed networks of functionally interconnected regions that emerge and dissolve over multiple timescales (Cabral, Kringelbach, & Deco, 2014, 2017; Calhoun, Miller, Pearlson, & Adalı, 2014; Deco, Jirsa, & McIntosh, 2011; Hutchison et al. 2013a; Kottaram et al., 2018; Preti, Bolton, & Van De Ville, 2016). An emerging idea is that of a functional repertoire of putative brain states that is continually revisited and rehearsed against a background of noise-driven endogenous neural activity (Deco & Jirsa, 2012; Sporns, 2013). The dynamics that play out on this functional repertoire are thought to support cognition (Cabral et al., 2017; Cocchi, Zalesky, Fornito, & Mattingley, 2013) and reflect the overall functional capacity of a neural system (Deco et al., 2011), which are likely related to changing mental states. Given that cognitive deficits are one of the core clinical features of schizophrenia (Bora & Pantelis, 2015; Elvevåg & Goldberg, 2000), and cognition is thought to emerge from the dynamic interactions among distributed brain regions (Bressler & Menon, 2010; Cabral et al., 2017; Cabral, Kringelbach & Deco 2017; Cocchi, Harding et al., 2014; Cole, Ito, Bassett, & Schultz, 2016), we hypothesized that neurocognitive and behavioral deficits associated with the disorder may be characterized by altered transition dynamics between putative brain states.

Previous studies suggest that large-scale neural dynamics in schizophrenia are aberrant and characterized by reduced dynamism (Damaraju et al., 2014; Miller et al., 2016), heritable (Su et al., 2016), distinguishable from bipolar disorder (Rashid et al., 2014) and healthy comparison individuals (Kottaram et al., 2018), and associated with working memory performance (Fu et al., 2017). These previous studies have primarily focused on characterizing functional connectivity dynamics (i.e., interregional coupling), rather than the dynamics of brain activity per se (i.e., blood-oxygenation level-dependent [BOLD] signal dynamics). While connectivity and activity are related, time-resolved analysis of functional connectivity is hampered by controversy in the core definition of connectivity dynamics (Liegeois, Laumann, Snyder, Zhou, & Thomas Yeo, 2017) and ongoing debate about choice of window lengths and other potential confounds (Hindriks et al., 2016; Leonardi & Van De Ville, 2015; Lindquist, Xu, Nebel, & Caffo, 2014; Zalesky & Breakspear, 2015). To circumvent these concerns, a more principled approach may be to explicitly model the dynamics of brain activity in regions or networks of interest.

One such computationally tractable model is the hidden Markov model (HMM). The basic premise of the HMM is that brain activity measurements from multiple locations can be decomposed into a sequence of discrete brain states that repeat over time. These putative brain states are continually revisited and represent distinct spatiotemporal patterns of activation, which are not directly observable, and thus considered "hidden." The HMM aims to discover these hidden brain states as well as the likely sequence of transitions between them. The overall proportion of time that an individual resides in each putative brain state, known as the state's *fractional occupancy*, and the average time spent in each state during each visit, known as the *mean lifetime* or *dwell time*, can then be inferred for each individual.

The HMM has recently been applied to model neural dynamics inferred from magnetoencephalography (MEG) (Baker et al., 2014; Quinn et al., 2018; Vidaurre et al., 2016) as well as task-based and resting-state functional MRI data (Ryali et al., 2016; Vidaurre et al., 2017a; Vidaurre et al., 2017b; Taghia et al., 2018). These seminal studies provide evidence for the utility of the HMM in characterizing dynamic interactions between brain networks in healthy individuals and show that the frequency of state transitions increases with age (Ryali et al., 2016) and transitions can be organized hierarchically into cognitive and sensorimotor metastates, with dwell times in these putative metastases being heritable and correlating with cognitive traits (Vidaurre et al., 2017a).

In the present study, we aim to model the temporal dynamics of neural activity in individuals with schizophrenia and investigate any potential relation between these dynamics and the disorder's core symptoms. We hypothesize that the clinical symptoms and pervasive cognitive deficits evident in schizophrenia may be associated with aberrant dynamics involving activation of the default mode, salience, executive control, and sensorimotor networks. To investigate this hypothesis, we fit an HMM to resting-state functional MRI data acquired in individuals with schizophrenia and healthy comparison individuals. Our study is the first to apply the HMM to a clinical population. We show that the HMM provides a principled characterization of how canonical brain networks are coupled and evolve over time in schizophrenia.

2 | MATERIALS AND METHODS

2.1 | Participants

Two neuroimaging data sets were analyzed. Data set 1 comprised individuals with schizophrenia and healthy comparison individuals, and was used to address the primary aims of this study. Data set 2 comprised only healthy individuals and was used to test the robustness and replicability of the HMM.

Data set 1: Detailed clinical assessment and neuroimaging of brain anatomy and function was performed in 41 individuals with schizophrenia (mean age 40.9 ± 10.0 years, 28 males) and 41 healthy comparison individuals (age-matched, mean age 38.3 ± 10.9 years, 24 males). Individuals with a confirmed diagnosis of schizophrenia

(DSM-IV) were recruited from inpatient and outpatient clinics in the metropolitan area of Melbourne, Australia. Individuals with schizophrenia were treatment-resistant, defined as at least two unsuccessful trials of at least two antipsychotic medications in the last 5 years. Exclusion criteria included any contraindication to MRI, any neurological disorder, history of brain trauma followed by a long period of amnesia, mental retardation, current drug or alcohol dependence, and/or history of electroconvulsive therapy. Healthy comparison individuals were recruited from the local community and had similar socio-economic backgrounds to that of patients. Healthy comparison individuals were excluded if they had a personal or family history of psychosis or bipolar disorder. All individuals were aged between 18 and 62 years and provided written informed consent before participation. Recruitment and all data acquisition procedures were approved by the Melbourne Health Human Research Ethics Committee (MHREC ID 2012.069). Demographics and clinical characteristics are shown in Table 1.

Data Set 2: Minimally preprocessed resting-state functional MRI data from the human connectome project (HCP; Smith et al., 2013) was sourced for 40 healthy adults (age range = 22–35 years; 20 males) to assess the robustness and replicability of the model. Details about recruitment procedures and inclusion/exclusion criteria are described in detail elsewhere (Van Essen et al., 2013).

2.2 | Clinical assessments

All individuals were administered the Mini International Neuropsychiatric Interview (Sheehan et al., 1998) to confirm diagnosis of individuals with schizophrenia and exclude current or past psychopathology in the healthy comparison individuals. Further, all individuals were administered the global assessment of functioning (GAF; Hall & Parks, 1995) and the social and occupational functioning assessment scale (SOFAS; Goldman, Skodol, & Lave, 1992). The scale for the assessment of positive symptoms (SAPS) and the scale for the assessment of negative symptoms (SANS; Andreasen, Flaum, Arndt, Alliger, & Swayze, 1991) were used to assess clinical symptoms in individuals with schizophrenia. The Cambridge neuropsychological test automated battery (CANTAB; Sahakian et al., 1988) was used to assess cognition (executive function and working memory) and the Wechsler abbreviated scale of intelligence (WASI; Wechsler, 1955) was used to measure full-scale intelligence quotient.

2.3 | Image acquisition

Data set 1: Data were acquired on a Siemens Avanto 3T Magnetom TIM Trio scanner. T1 weighted images of brain anatomy were acquired using an optimized Magnetization-Prepared Rapid acquisition Gradient Echo sequence (176 sagittal slices with 1 mm thickness without gap; repetition time (TR) = 1980 ms; echo time (TE) = 4.3 ms; flip angle = 15°; field of view (FOV) = 250 × 250 mm^2 and resolution = 0.98 × 0.98 × 1.0 mm^3). Resting-state functional images were acquired using a T2*-weighted echo-planar imaging sequence (TR = 2 s, TE = 40 ms, voxel dimensions = 3.3 × 3.3 × 3 mm^3 and matrix size 64 × 64), for a duration of 7.8 min, resulting in 234 frames. Individuals were instructed to stay awake and keep their eyes closed during the scan.

Data set 2: Acquisition details are described in detail elsewhere (Smith et al., 2013). In short, 1,200 frames of resting-state multiband, gradient-echo planar imaging were acquired during a period of 14.4 min with the following parameters: relaxation time, 720 ms; echo time, 33.1 ms; flip angle, 52°; field of view, 280 × 180 mm; matrix, 140 × 90; and voxel dimensions, 2 mm isotropic. Only one of the four runs acquired for each individual was analyzed in this study (left–right encoded, first session).

2.4 | Image preprocessing

Data set 1: Image preprocessing was performed using FSL (FMRIB software Library, https://fsl.fmrib.ox.ac.uk/fsl/) and SPM8 (www.fil.ion.ucl.ac.uk/spm). The following sequence of steps was completed

TABLE 1 Demographic, behavioral, and clinical characteristics (Data set 1)

	Schizophrenia (n = 41)	Comparison group (n = 41)	Between-group comparison
Sex (male/female)	28/13	24/17	$\chi^2(1, N = 82) = 0.97, p = 0.32$
Age (years)	40.9 ± 10.0	38.3 ± 10.5	$t(82) = 1.1, p = 0.27$
Illness duration (years)	17.9 ± 9.3	–	–
IQ (WASI)	86.1 ± 18.7	111.2 ± 13.6	$t(75) = 6.70, p < 0.01*$
Education (years)	12.0 ± 0.55	16.4 ± 0.47	$t(79) = -6.35, p < 0.01*$
GAF	45.9 ± 13.0	79.5 ± 10.6	$t(79) = -12.79, p < 0.01*$
SOFAS	46.5 ± 14.8	79.5 ± 11.0	$t(80) = -11.49, p < 0.01*$
Generalized cognition[1] (CANTAB)	−48.5 ± 30.2	42.9 ± 20.7	$t(82) = 7.91, p < 0.01*$
Clozapine dosage (mg/day)	393.24 ± 24.6	–	–
Chlorpromazine equivalent dosage (mg/day)	615.4 ± 55.84	–	–
SAPS[2]	1.19 ± 0.62	–	–
SANS[2]	1.48 ± 0.79	–	–

Note. IQ = intelligence quotient; WASI = Wechsler abbreviated scale of intelligence; GAF = the global assessment of functioning; SOFAS = social and occupational functioning assessment scale; CANTAB = Cambridge neuropsychological test automated battery; SAPS = scale for the assessment of positive symptoms; SANS = scale for the assessment of negative symptoms; mg = milligram.
*Significant p < 0.01. Mean ± standard deviation of each measure is shown.
[1]Principal component across multiple CANTAB outcome measures (Section 2.8, Supporting Information Table S2).
[2]Mean across all available subscales (Section 2.8, Supporting Information Table S2). Variation in degrees of freedom is due to missing data for some individuals.

for each individual: slice-time correction, realignment to the mean functional volume to correct for head motion, co-registration to the respective T1-weighted anatomical image via rigid-body registration and then spatial normalization to the Montreal Neurological Institute 152 template maintaining an isotropic 2 mm resolution via nonlinear transformation. Confounds such as motion parameters (Friston 24-parameter model; Friston, Williams, Howard, Frackowiak, & Turner, 1996) and signals from white matter and ventricles were regressed from the BOLD time courses for each gray matter voxel, to correct for head motion and physiological noise. Spatial smoothing was applied to the residuals from this regression using a Gaussian kernel of full-width at half-maximum (FWHM) of 4 mm. After smoothing, the voxel time courses were band-pass filtered (0.01–0.1 Hz) to alleviate low-frequency drifts and high-frequency physiological noise (Cordes et al., 2001). Global signal regression was not applied, given that this procedure has been suggested to alter the covariance structure of the data (Murphy, Birn, Handwerker, Jones, & Bandettini, 2009), particularly when assessing dynamics (Xu et al., 2018).

Of note, the sample characterized in Table 1 excludes seven individuals (three healthy and four schizophrenia individuals) who were omitted due to excessive intrascan head motion (framewise displacement [FD] >0.5 mm). For the remaining individuals, FD did not significantly differ ($p > 0.05$) between the schizophrenia group (0.14 ± 0.07 mm) and healthy comparison individuals (0.1 ± 0.05 mm).

Data set 2: The minimal preprocessing pipeline for the HCP data is described in detail elsewhere (Smith et al., 2013). The minimally preprocessed data were spatially smoothed with a Gaussian kernel (FWHM = 4 mm) and band-pass filtered (0.01–0.1 Hz). These additional steps were undertaken to ensure Data sets 1 and 2 shared comparable frequency spectra and spatial smoothness.

2.5 | Delineation of resting-state networks

The temporal dynamics of BOLD activity were modeled in 14 canonical resting-state networks (RSNs) using a HMM. The spatial extent of each RSN was delineated according to established reference maps (Shirer, Ryali, Rykhlevskaia, Menon, & Greicius, 2012; Supporting Information Table S1). RSNs included cortical, subcortical, and cerebellar regions. For each individual, network-averaged time courses were determined for each of the 14 RSNs by averaging BOLD activity over all voxels encapsulated by the RSN. These time courses were normalized to have zero mean and unit standard deviation across time. Normalization was performed separately for each RSN and each individual. These steps yielded a matrix with three dimensions: subjects × RSNs × time (Data set 1: 82 × 14 × 234; Data set 2: 40 × 14 × 1,200). The RSNs could have been alternatively delineated using independent component analysis (ICA) or other data-driven parcellation methods; but this would limit the comparability of the model across data sets. Hence, we opted to use established reference maps that facilitate these explicit comparisons.

2.6 | Hidden Markov model

The network-averaged BOLD time courses for each RSN (zero mean and unit standard deviation) were temporally concatenated across all individuals with schizophrenia as well as healthy comparison individuals. After concatenation, the three dimensional matrix was thus reduced to two dimensions: RSNs × T, where T = subjects × time (Data set 1: 14 × 19,200; Data set 2: 14 × 48,000). The HMM was then fitted to the temporally concatenated time courses. Fitting the HMM to the concatenated data yielded a single set of model parameters (e.g., brain states) that represented a consensus across all individuals. While all individuals thus shared a common set of states, the amount of time spent in each state and the transition probabilities between states varied between individuals.

A schematic of the HMM architecture used in the present study is shown in Figure 1 and a brief technical overview of the HMM is provided in Supporting Information Section 1. The basic premise of the HMM is that BOLD activity dynamics in the 14 RSNs can be decomposed into a sequence of discrete brain states that repeat over time. These putative brain states represent distinct spatiotemporal patterns of activation. For example, a certain state might be characterized by relatively high activity in the default mode RSNs and relatively low activity in all other RSNs, potentially corresponding to an introspective state. The HMM aims to discover these hidden brain states as well as the likely sequence of transitions between the states, under the assumption that the network-averaged BOLD time courses are stationary processes and the probability of the current state only depends on the previous state.

The HMMBOX MATLAB toolbox (www.robots.ox.ac.uk/~parg/software) was used to perform variational Bayes (VB) inference on the HMM (Rezek & Roberts, 2005). Further details about VB inference on HMMs are available elsewhere (Baker et al., 2014; Vidaurre et al., 2017a). A total of 400 training cycles were completed and the model fit with the lowest free energy was selected. A multivariate Gaussian distribution was chosen for the observation model (emission distribution), and thus each inferred state was fully characterized by a mean activation for each RSN ($K \times 1$ vector per state; Figure 1c) as well as a $K \times K$ covariance matrix, where K denotes the number of RSNs ($K = 14$ in this study). Covariance matrices were not analyzed in this study. The group-level transition probability matrix was also estimated (Figure 1d). Element (i, j) of the transition matrix is the probability of transitioning from the state x_i to state x_j, while element (i, i) relates to the average amount of time spent in state x_i. Because we used a VB inference framework, the marginal posterior distribution on the state variable was estimated, and thus to compute summary statistics, the most probable a posteriori state was chosen to be the active state at each time point (Figure 1e).

The total number of states comprising the HMM needs to be specified a priori. Previous studies that modeled functional MRI dynamics in healthy individuals have considered 5–12 states (Baker et al., 2014; Damaraju et al., 2014; Ou et al., 2015; Vidaurre et al., 2017a). Following the recent study of Vidaurre et al. (2017a), we foremost inferred an HMM with $M = 12$ states. Our results were qualitatively comparable for HMMs inferred with as few as eight states. Moreover, HMMs comprising 8–12 states differed negligibly in goodness of fit (Supporting Information Figure S1). Inference with 12 states yielded the most physiologically plausible findings and provided a marginally improved fit (free energy).
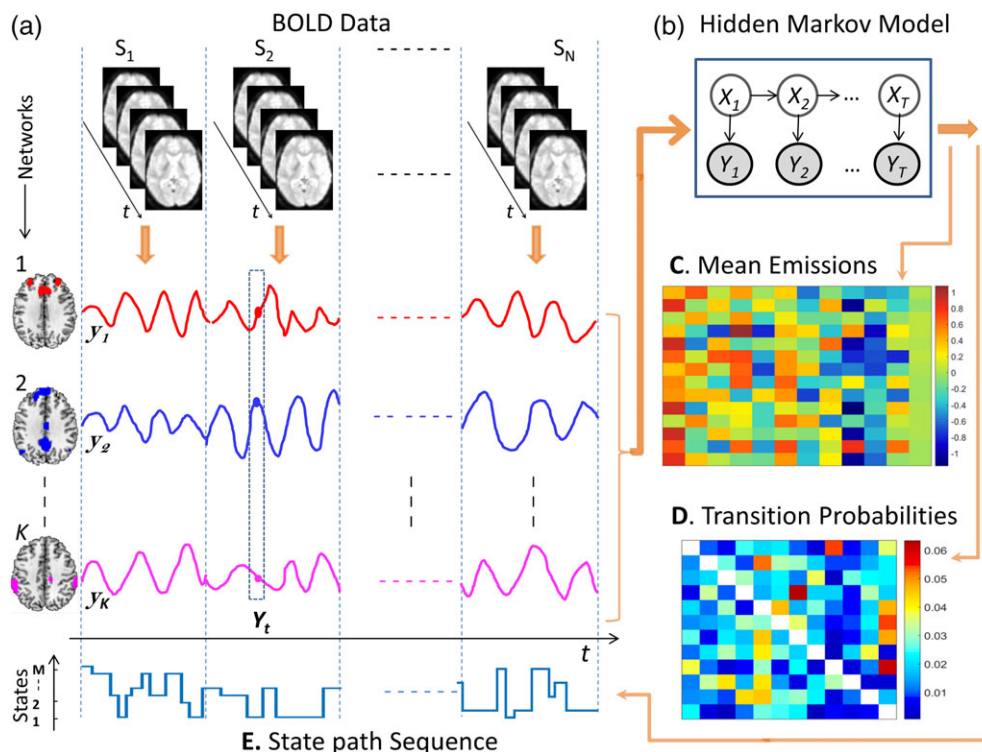
FIGURE 1 Architecture of the HMM. (a) HMM inputs were network-averaged BOLD time courses for each of K RSNs. Network-averaged time courses were temporally concatenated across N individuals (columns), where the dashed vertical lines indicate concatenation points. Concatenated time courses are denoted y_k, k = 1, ... K. (b) The HMM identified recurring patterns of activation among the K network-averaged time courses. Each distinct activation pattern was assumed to represent a putative brain state. The variable $X_t \in \{x_1, x_2, ... , x_M\}$ denotes the state in which the brain resides at time t, where M is the total number of states comprising the HMM, while the variable $Y_t = (y_{1,t}, y_{2,t}, ... , y_{K,t})$ denotes the values of the network-averaged time courses observed at time t. The variable X_t is not directly observable from the data, and is thus considered 'hidden'. According to the HMM, the brain resides in a given state for a certain period of time and then transitions to a new state with a probability that depends only on the previous state. At time t, the value of the observed variable Y_t depends only on the value of the state X_t and was assumed to follow a K-variate Gaussian distribution in this study. The parameters fitted to the HMM are: i) the mean activity of the RSNs in each state (emission distribution parameters, Panel C); and, ii) the probabilities of transitioning from one state to another (transition probabilities, Panel D). (C) Example fit of emission distribution means for each of M = 12 brain states (columns). Element (i, j) of the matrix is the mean activity of RSN i in state j. (D) Example matrix of transition probabilities, where element (i, j) is the probability of transitioning to state x_j from state x_i. (E) After fitting the HMM, the most probable brain state at each time point for each individual was inferred using Viterbi decoding. The state path sequence shown contains discrete steps of varying height, each of which corresponds to a state transition. Brain states are labeled with integers in an arbitrary order (vertical axis). Note that the HMM infers a covariance matrix corresponding to each state; however this was not analyzed in the present study; hence not listed here [Color figure can be viewed at wileyonlinelibrary.com]

2.7 | Inference

After the HMM was inferred, each individual was characterized by a distinct transition probability matrix ($M \times M$) as well as distinct fractional occupancy ($M \times 1$) and mean lifetimes ($M \times 1$) for each of the M = 12 states. These descriptors were derived from the state path sequence for each individual (Figure 1e). Transition probabilities characterized the probability of transitioning from one state to another at each time epoch. Each time epoch corresponded to one TR. A state's *fractional occupancy* was defined as the proportion of time that an individual resided in the state during the scan acquisition, whereas the state's *mean lifetime*, or *dwell time*, was the average time an individual resided in the state during each visit (Baker et al., 2014). Fractional occupancy and mean lifetimes provided complementary characterizations: states with long fractional occupancy times, but short mean lifetimes, are frequently visited for short intervals.

Inference was performed to evaluate the null hypothesis of equality in transition probabilities, fractional occupancy times, and mean

lifetimes between the schizophrenia and healthy comparison groups. The network-based statistic (NBS) (Zalesky, Fornito, & Bullmore, 2010) was used to perform inference on the transition probability matrices. The primary statistic threshold was set to 2.5; a total of 5,000 permutations were generated; and the family-wise error rate was controlled at 5%. Connected components in the network of supra-threshold connections were identified with a breadth first search and the size of each connected component was measured based on the number of supra-threshold connections it comprised. Permutation testing was performed by shuffling group labels (schizophrenia or control) among individuals, under the assumption of exchangeability. For each permutation, the size of the largest connected component was stored to estimate an empirical null distribution. The family-wise error corrected p-value for a component of given size was then estimated as the proportion of permutations with components of equal or larger size.

Two-sample t-tests were used for fractional occupancy and mean lifetimes and permutation testing was used to assess the null

hypothesis of equality in fractional occupancy and mean lifetimes between the schizophrenia and healthy comparison group. Specifically, we generated 5,000 permutations by shuffling group labels (schizophrenia or control) among individuals. For each permutation, a *t*-statistic was computed to test for a between-group difference in fractional occupancy or mean lifetimes. The absolute value of the *t*-statistic was stored for each permutation, thereby generating an empirical null distribution. A separate null distribution was estimated for each state. The *p*-value for each state was then estimated as the proportion of samples in the state's null distribution that were greater than or equal to the absolute value of the *t*-statistic in the nonpermuted data.

2.8 | Canonical correlation analysis

Canonical correlation analysis (CCA) was used to study associations among clinical/behavioral measures and fractional occupancies of different states in schizophrenia individuals. CCA enabled discovery of multivariate associations between state descriptors of the HMM and interindividual variation in clinical/behavioral measures, thereby providing a more principled approach than independently assessing each potential association and then correcting for multiple tests. Specifically, CCA tested for multivariate associations across individuals between the 12 fractional occupancy times and 8 measures characterizing positive (SAPS) and negative symptoms (SANS), general (GAF) and social (SOFAS) functioning, full-scale intelligence quotient (WASI), a generalized measure of cognition (based on the CANTAB), chlorpromazine equivalent dosage as well as the illness duration. Further details on each score can be found in Supporting Information Table S2. Principal component analysis was applied to summary measures to estimate missing values. CCA was performed on the resultant measures and the fractional occupancy times of 12 states. Permutation testing was performed to establish significance of the correlation. The fractional occupancy times were randomly permuted between individuals and the CCA was re-estimated using this permuted data. The correlation coefficient associated with the principal canonical mode was then stored. This was repeated for 5,000 independent permutations, thereby generating an empirical null distribution. A familywise error corrected *p*-value was computed for each canonical mode in the unpermuted data as the proportion of correlation coefficients in the null distribution that either equaled or exceeded the correlation coefficient associated with the mode.

2.9 | Prediction of diagnostic status

Machine classifiers were trained to classify individuals according to diagnostic status (schizophrenia or control) based on the fractional occupancy times for each of the 12 states inferred from the HMM. Ten-fold cross-validation (CV) was used to evaluate the performance of each classifier as follows. Data set 1 was randomly partitioned into two mutually exclusive groups of individuals—one containing 90% of the sample and the other with the remaining 10% of individuals. The HMM with 12 hidden states was inferred using individuals comprising the larger partition (90%) and the state path sequences for each individual were estimated. The HMM fitted to the larger partition was then used to estimate the state path sequences for each individual

comprising the smaller partition (10%). Note that the HMM was not re-fitted to the data comprising the smaller partition. Fractional occupancy times were then computed for each state and each individual. The 12 fractional occupancy times computed for each individual were used as features for machine classification of diagnostic status. The following classifier models were investigated: (a) support vector machines (SVM) with a linear kernel, (b) *k*-nearest neighbor (*k* = 5), (c) decision trees, (d) naive Bayes, (e) random forests, and (f) ensemble method (via boosting of trees). Each classifier model was trained on the larger partition and then used to predict single-subject diagnosis in the remaining 10% of the sample. Classifier performance was assessed using accuracy, sensitivity, specificity, and area under the curve (AUC). The 10-fold CV was repeated 100 times to estimate the average performance under a range of data partitions.

In supplementary analyses, we investigated the robustness and replicability of the states inferred by the HMM using an independent data set (Data set 2) comprising healthy individuals (Supporting Information Section 2).

3 | RESULTS

The HMM architecture shown in Figure 1 (12 states) was used to model resting-state functional MRI dynamics in 14 canonical RSNs. The spatiotemporal characteristics of these dynamics were then: (a) investigated for aberrant behavior in individuals with schizophrenia (*n* = 41), relative to healthy comparison individuals (*n* = 41); (b) tested for associations with the severity of clinical symptoms and cognitive deficits; (c) evaluated as features to predict single-subject diagnostic status using a range of machine classifiers; and (d) compared to an independent data set to establish the robustness of the HMM.

3.1 | Characterization of brain states

The 12 putative brain states inferred from the HMM are characterized in Figure 2 and represent recurring patterns of activation among the 14 RSNs. The data used to infer the HMM were normalized to have zero mean and unit standard deviation across time, and thus an activation of zero in Figure 2 corresponds to the mean level of activation. Accordingly, negative activations (cool colors) indicate a relatively low level of BOLD activity (i.e., below average), while positive activations (warm colors) indicate relatively high BOLD activity (i.e., above average). State *Hi* is an aroused state in which all RSNs are active, whereas state *Lo* is the converse state in which all RSNs show dampened activity. Similarly, states DM*Lo*-Sen*Hi* and DM*Hi*-Sen*Lo* demonstrate antagonistic behavior between the default mode and sensory networks. State *Mean* is the baseline state in which all RSNs exhibit their mean level of activation. States are also evident where salience and executive networks show high and/or low activity (Sal*Hi*-Ex*Hi*, Sal*Lo*-Ex*Hi*, and DM*Hi*-Sal*Lo*).

The covariance matrix inferred for each state is shown in Supporting Information Figure S4. In this study, no further analysis was performed on the covariance matrices.
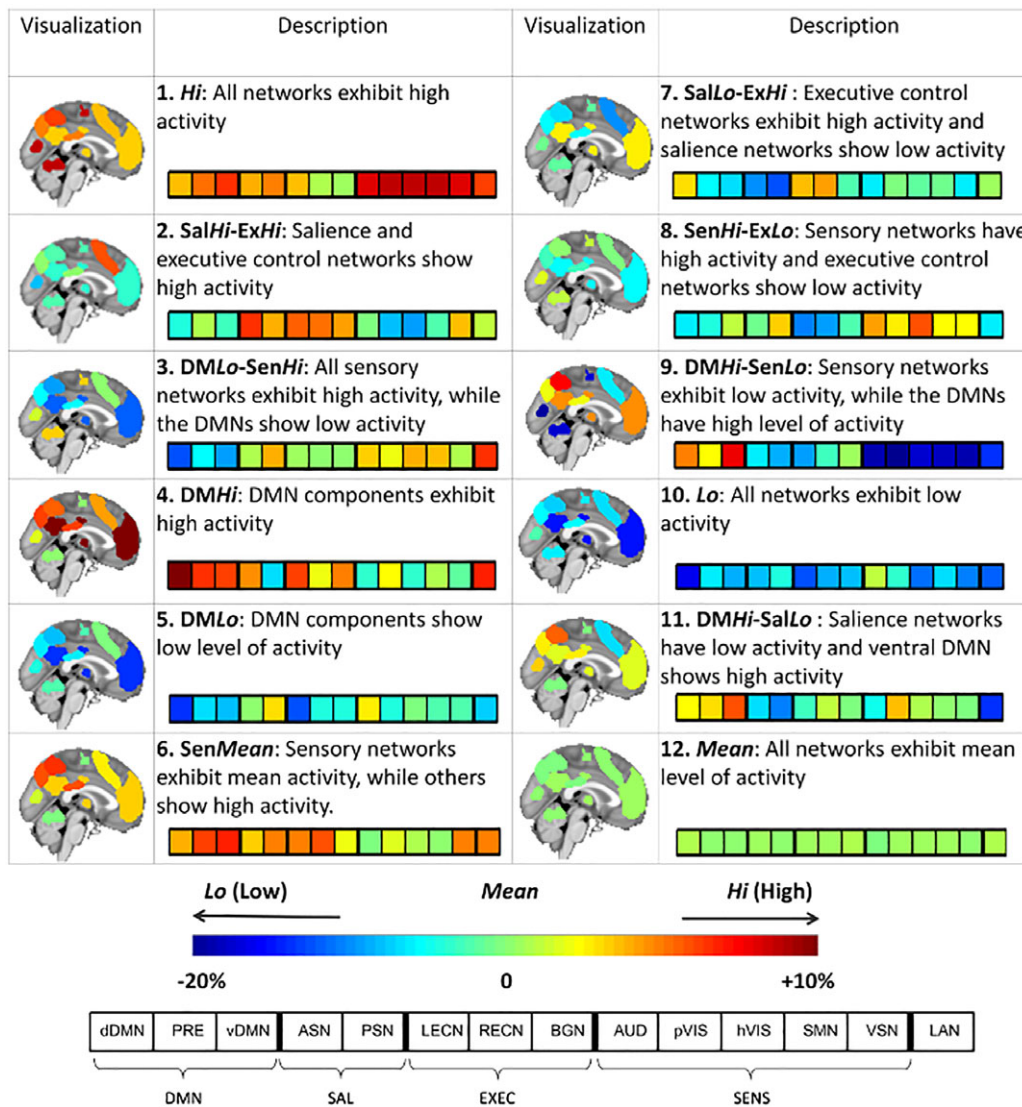
FIGURE 2 Characterization of inferred brain states. A HMM was used to decompose functional MRI dynamics in 14 predefined RSNs into a sequence of 12 repeating brain states. Brain activation maps illustrate the level of normalized BOLD activity within the regions comprising each RSN. The 12-segment bar provides a summary of the activation pattern characterizing each state. Data used to infer the HMM were normalized, and thus an activation of zero corresponds to the mean level of activation (green shades). The activation of each RSN is expressed as a percentage above or below the mean level of activation. DMN, default mode networks; SAL, salience networks; EXEC, executive control networks; SENS, sensory networks. Supporting Information Table 1 provides details about the 14 RSNs [Color figure can be viewed at wileyonlinelibrary.com]

3.2 | Aberrant dynamics in schizophrenia

Between-group inference was performed on three summary measures characterizing the dynamic behavior of the HMM: (a) state transition probabilities (12×12 matrix per individual); (b) proportion of time spent in a state, or fractional occupancy (12 occupancies per individual); and (c) average time spent in a state during each visit, or mean lifetime (12 lifetimes per individual). Figure 3 shows the mean fractional occupancies (Panel a) and mean lifetimes (Panel b) for each group of individuals and each of the 12 states. Fractional occupancy times for each individual are reported in Supporting Information Figure S5. Relative to the healthy comparison group, individuals with schizophrenia resided for significantly shorter periods in states characterized by: (a) overall high activation (*Hi*); and (b) relatively high activation of the default mode network (DMN) and diminished activation of

sensory networks (DM*Hi*-Sens*Lo*). In particular, the fractional occupancy of state DM*Hi*-Sens*Lo* is 5–6% lower in patients. Despite residing in this state for significantly shorter periods than the comparison group, this state's mean lifetime was significantly increased (4–5 s on average) in the schizophrenia group. Therefore, schizophrenia is characterized by infrequent but prolonged visits to state DM*Hi*-Sens*Lo*. Furthermore, the schizophrenia group resided for significantly longer periods in states that were characterized by: (a) low overall activation (*Lo*); and (b) heightened activation of sensory networks combined with relatively low activation of cognitive and executive control networks (DM*Lo*-Sens*Hi* and Sens*Hi*-Ex*Lo*).

Figure 4a shows group-averaged transition probability matrices. The top 20% of these transitions are visualized as a state transition diagram in Figure 4b. It must be noted that these transitions do not
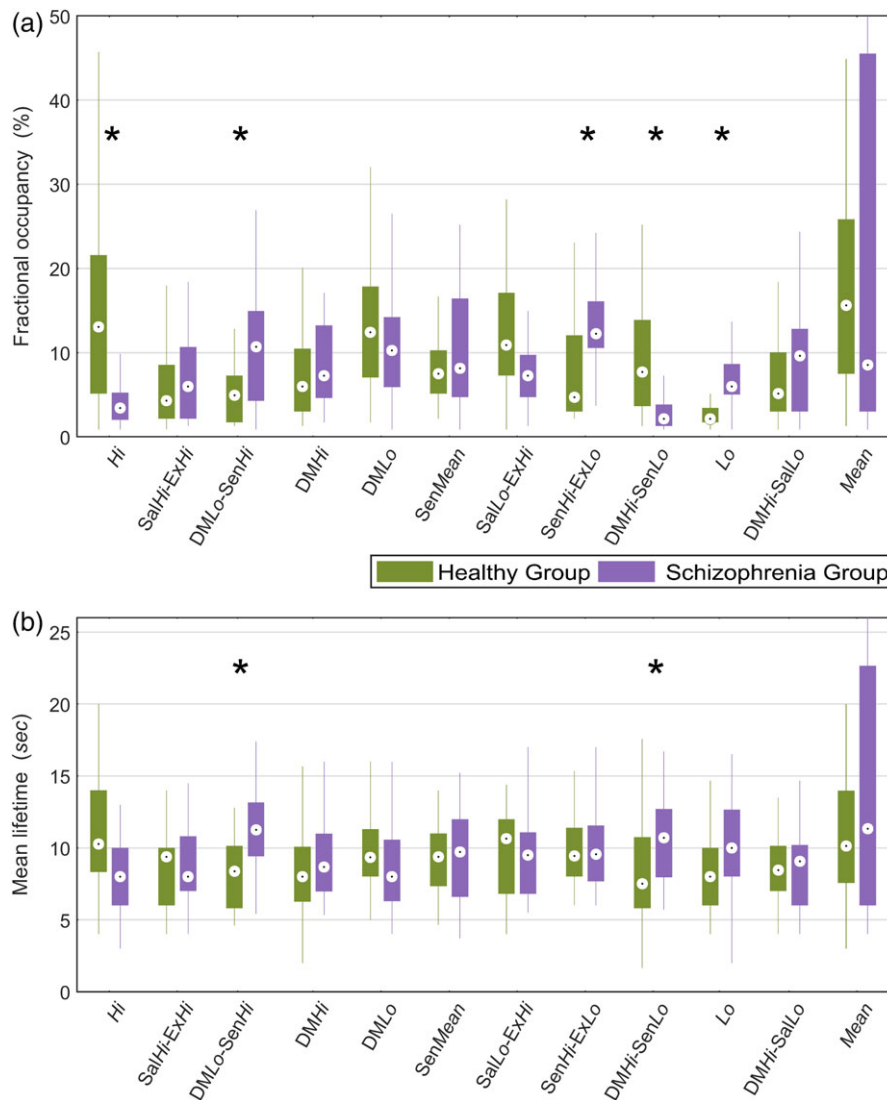
FIGURE 3 Comparison of fractional occupancy and mean lifetimes between schizophrenia and healthy comparison groups for states inferred from the HMM. (a) Comparison of fractional occupancy times for each of the 12 states inferred from the HMM. A state's fractional occupancy is the proportion of time that an individual resided in the state during the scan acquisition. (b) Comparison of mean lifetimes for each state. A state's mean lifetime is the average time an individual resided in the state during each visit. Permutation tests (Section 2.7) were performed to assess the null hypothesis of equality in fractional occupancy times between the schizophrenia and healthy comparison group. Asterisks (*) denote $p < 0.05$. Boxplots: upper (lower) box edge, 25th (75th) percentile; central dot, median; thin lines, 1.5 x interquartile length [Color figure can be viewed at wileyonlinelibrary.com]

imply significant between-group differences; rather, they are more probable on average. Significant between-group differences in transition probabilities were found with the NBS ($p < 0.05$) and these transitions are shown in Figure 4c. Note that the NBS can detect individual connections (i.e., components of size one) if the majority of permutations (i.e., >95%) do not contain any connections that exceed the primary statistic threshold, leading to a null distribution predominated by components of size zero. Several observations about the sequence of transitions between states warrant consideration. First, the healthy comparison group tends to transition back and forth between states *Hi* and DM*Hi*-Sens*Lo* (1↔9 loop). In contrast, this putative loop is absent in the schizophrenia group, where state *Mean* is the preferred transition from both these states. Second, healthy individuals are more likely to transition to state DM*Hi*-Sens*Lo* from state *Lo* (10 → 9), whereas schizophrenia individuals often transition

back and forth between states *Lo* and DM*Lo*-Sens*Hi* (10 ↔ 3). Third, from state DM*Hi*-Sal*Lo*, healthy individuals preferably transition to states *Hi* or DM*Lo* (11 → 1/5), whereas individuals with schizophrenia are more likely to transition to state DM*Hi* (11 → 4). Together, these results suggest that schizophrenia is characterized by an inability to dynamically activate and deactivate the DMN.

3.3 | Association between aberrant dynamics and clinical symptoms

Fractional occupancy times were associated with the largest effect sizes (Figure 3a), and were thus selected as the summary measure to correlate with the severity of clinical symptoms and cognitive deficits in the schizophrenia individuals. CCA identified one significant mode ($r = 0.9$, $p < 0.01$, family-wise error corrected across all CCA modes
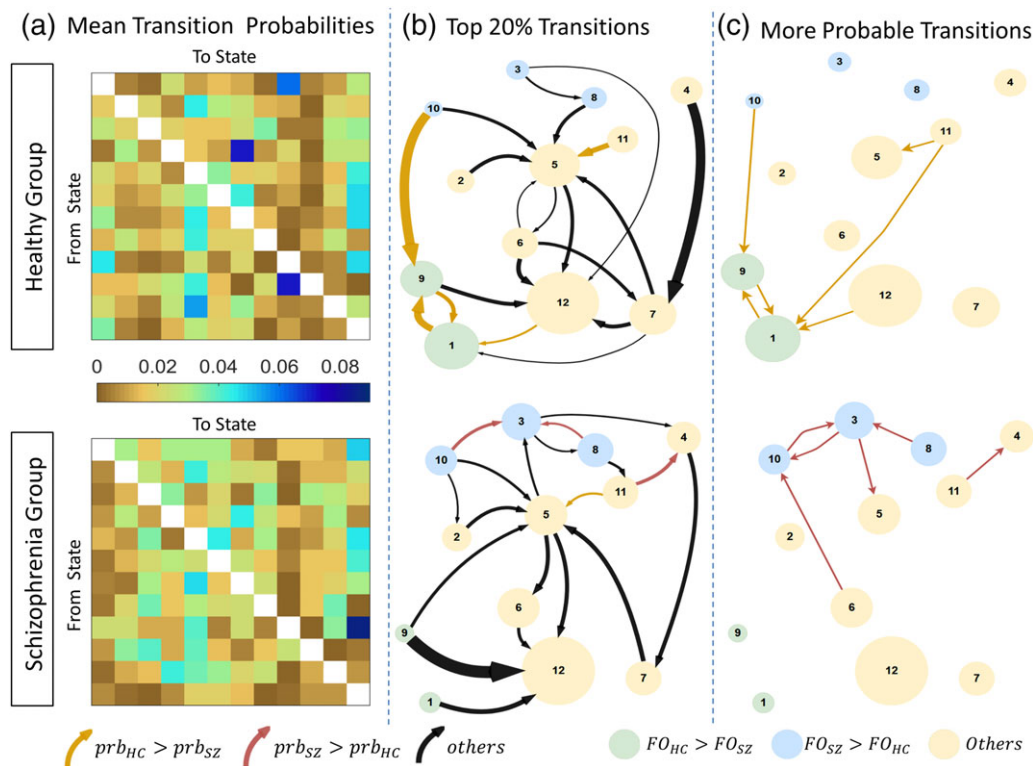
FIGURE 4 Transition probabilities between brain states for schizophrenia and healthy comparison groups. (a) Group-averaged transition probability matrices for schizophrenia (lower) and healthy comparison groups (upper). Diagonal matrix elements omitted to aid visualization. (b) Top 20% of the transitions (c) State transitions that have significantly different probability of occurrence ($p < 0.05$), identified by network-based statistic. Each circle represents a state. Circle diameter is modulated by the fractional occupancy time of the corresponding state. Circle colors denote states with significantly increased fractional occupancy in the healthy comparison (green) and schizophrenia (blue) groups. Yellow circles denote states with no significant between-group difference in fractional occupancy. Each arrow represents a transition. Arrows denote transitions with significantly greater probability in healthy comparison (dark yellow) and schizophrenia (maroon)) groups. Arrow thicknesses in panel b correspond to group-averaged probability of that transition. The 20% strongest transitions should not be interpreted as significant, but are rather visualized in panel b to highlight those transitions which are more probable on average. FO, fractional occupancy; Prb, probability. The 12 states are as follows: 1 = *Hi*, 2 = Sal*Hi*-Ex*Hi*, 3 = DM*Lo*-Sen*Hi*, 4 = DM*Hi*, 5 = DM*Lo*, 6 = Sen*Mean*, 7 = Sal*Lo*-Ex*Hi*, 8 = Sen*Hi*-Ex*Lo*, 9 = DM*Hi*-Sen*Lo*, 10 = *Lo*, 11 = DM*Hi*-Sal*Lo*, 12 = *Mean* [Color figure can be viewed at wileyonlinelibrary.com]

with permutation testing), which characterized an association between interindividual variation in positive symptoms and fractional occupancy times (Figure 5). Figure 5b shows that the canonical coefficient for the measure of positive symptoms (SAPS) is substantially greater than all other symptoms and cognitive measures. The significant CCA mode is thus predominantly explained by interindividual variation in positive symptoms. The canonical coefficients for the fractional occupancy times (Figure 5c) show a more complex pattern. In particular, the most positive canonical coefficients are associated with states DM*Lo*, Sen*Hi*-Ex*Lo*, and *Lo*, while states *Hi* and DM*Hi* show the most negative canonical coefficients. Therefore, the greater the severity of positive symptoms, the longer the proportion of time spent in states characterized by inactive default mode and executive networks, together with heightened activity in sensory networks.

3.4 | Prediction of diagnostic status

Six distinct machine classifiers were trained to predict the diagnostic status of each individual (schizophrenia or control) based on the 12 fractional occupancy times. Figure 6 shows classifier performance. For each classifier architecture, the accuracy, sensitivity, specificity, and AUC from 100 runs of 10-fold CV are reported. Classification

accuracies ranging between 76 and 85% were achieved across the six classifiers (sensitivity: 70–78%; specificity: 78–88%, area under curve: 75–82%). All performance measures are significantly greater than the chance level and multiple classifiers such as SVM, naive Bayes, random forest, and ensemble of trees provide a median accuracy above 80%, over different runs of 10-fold CV.

3.5 | Model robustness

Supplementary analyses show that the states inferred from the HMM are robust to the choice of initial conditions and stochastic variations in the training cycle (Supporting Information Figure S2). The states inferred from different instantiations of null data were observed to be substantially different from that inferred on the real data. The inferred states were also replicated in an independent group of healthy individuals (Supporting Information Figure S3). We observed that the state occupancy patterns of healthy individuals from Data sets 1 and 2 are positively correlated on average, whereas the occupancy patterns of schizophrenia individuals showed a slightly negative correlation, on average, to the occupancy patterns of healthy subjects from either data sets.
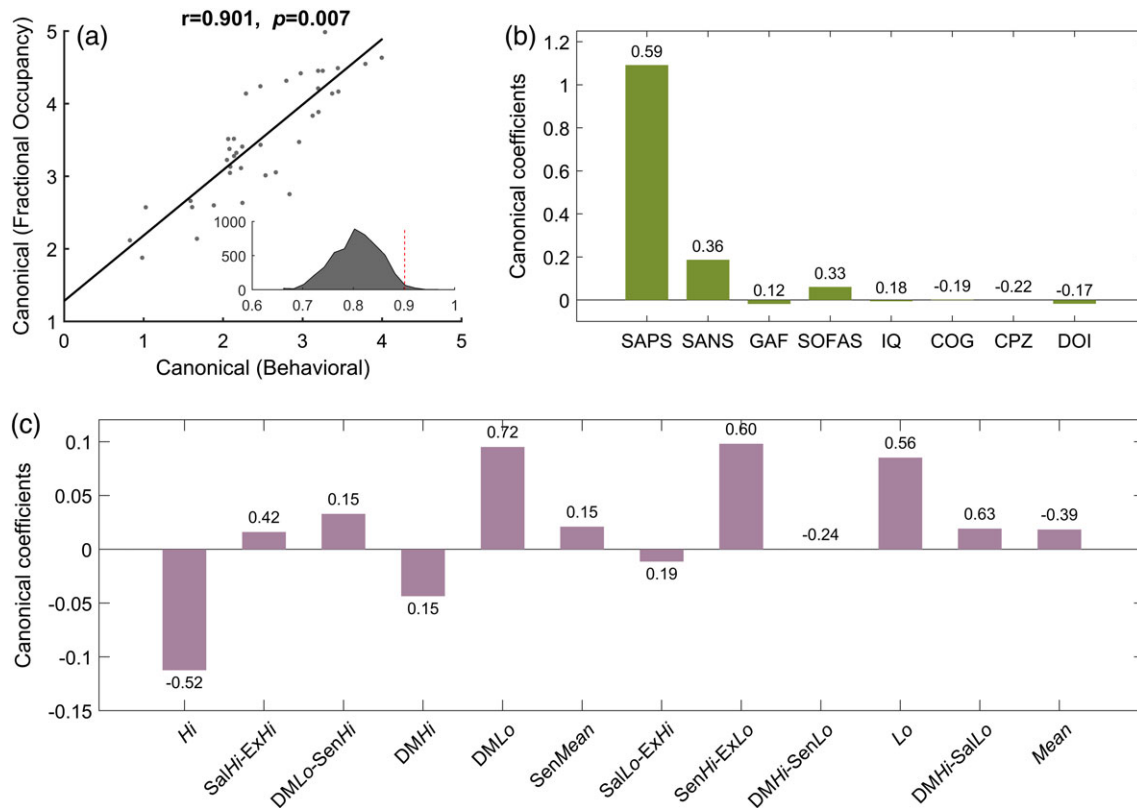
FIGURE 5 Association between interindividual variation in fractional occupancy times and severity of clinical symptoms and cognitive deficits. CCA was performed to test for multivariate associations between interindividual variation in fractional occupancy times for 12 brain states and eight measures of symptom severity, cognition, and clinical characteristics. (a) Scatter plot of canonical scores for the significant CCA mode. Solid black line denotes line of best fit. A correlation of 0.91 (p = 0.007, family-wise error corrected) was observed between the canonical covariates. The inset shows the distribution of correlation coefficients across 5,000 null instantiations (mean = 0.8). The dotted red line represents the observed correlation coefficient of 0.91, which is significant (p < 0.01) with respect to the null distribution. (b) Canonical coefficients corresponding to the eight summary measures. These measures are described in Supporting Information Table S2. SAPS, scale for the assessment of positive symptoms; SANS, scale for the assessment of negative symptoms; GAF, global assessment of functioning; SOFAS, social and occupational functioning assessment scale; IQ, intelligence quotient; COG, a generalized measure of cognition; CPZ, chlorpromazine equivalent dosage; DOI, duration of illness. (c) Canonical coefficients corresponding to fractional occupancy times of the 12 states. Figure 2 provides a description of each state. The value indicated above/below each bar indicates the Pearson correlation coefficient between the corresponding variable and its canonical covariate. Whereas the height of each bar indicates the extent to which each variable is up- or down-weighted in relation to its canonical covariate, the correlation coefficients provides a univariate measure of how strongly each variable is associated with its canonical covariate [Color figure can be viewed at wileyonlinelibrary.com]

4 | DISCUSSION

Schizophrenia is associated with disturbances to the activity and connectivity of brain networks, at rest (Calhoun et al., 2009; Breakspear et al., 2003; Liang et al., 2006; Fox & Greicius, 2010; Liu et al., 2006; Liu et al., 2008; Bluhm et al., 2007; Bluhm et al., 2009; Salvador et al., 2007; Zhou et al., 2007; Jafri et al., 2008; Whitfield-Gabrieli et al., 2009) and during the execution of cognitive and motor tasks (Calhoun et al., 2012; Gur et al., 2002; Harrison, Yücel, Pujol, & Pantelis, 2007; Hugdahl et al., 2004; Manoach et al., 1999; Yoon et al., 2008). In this study, we provided a novel characterization of these disturbances by explicitly modeling the dynamics of neural activity as a function of time, whereas most previous functional neuroimaging studies of schizophrenia have focused on static characterizations of activation and connectivity that represent time averages over the entire data acquisition interval. Time-resolved analyses of functional connectivity in schizophrenia suggest that the disorder is characterized by reduced dynamism in connectivity (Miller et al., 2016), shorter dwell times in

highly integrated states and altered thalamo-sensory dynamics (Damaraju et al., 2014). Furthermore, aberrant connectivity dynamics in the disorder are heritable (Su et al., 2016) and enable accurate, single-subject prediction of diagnostic status (Kottaram et al., 2018). These previous studies provided motivation to explicitly model the dynamics of fMRI activity in schizophrenia to gain deeper insight into the temporal characteristics of aberrant neural activity in the disorder.

To this end, we inferred an HMM from resting-state fMRI data that was temporally concatenated across adults with schizophrenia and healthy comparison individuals. The basic premise of the HMM inferred in this study was that fMRI activity within 14 canonical RSNs could be decomposed into a repertoire of 12 putative brain states, where each state characterized a distinct pattern of activation across the 14 networks. Neural dynamics under the HMM consisted of dwelling in a state for a period of time and then transitioning to a new state with a probability that only depended on the previous state. States were therefore continually revisited. For each individual, we quantified the proportion of time spent in each state (fractional
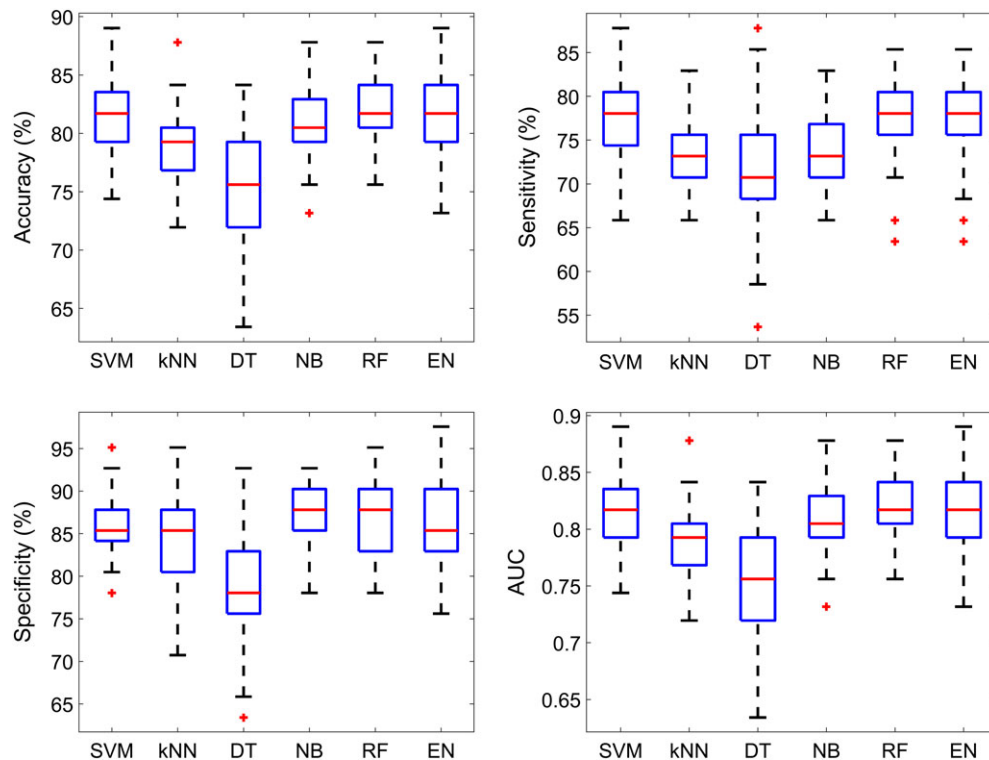
FIGURE 6 Box plots of different performance measures from single-subject prediction of diagnostic status. The 12 state fractional occupancy values were used as subject-specific features. Each box represents the distribution of a performance measure over 100 runs of 10-fold cross validation. Blue box = 25–75 percentile, red line = median, black dotted lines = 9–91 percentile, red "+" = outliers. AUC, area under the curve; SVM, support-vector machine; kNN, k-nearest neighbor; DT, decision trees; NB, naive Bayes; RF, random forest; EN, ensemble of trees [Color figure can be viewed at wileyonlinelibrary.com]

occupancy) and the average duration of visits to each state (mean lifetime) as well as the likelihood of transitioning from one state to another (transition probability matrix). These descriptors of the HMM were compared between the two groups and investigated for associations with symptom severity and cognitive deficits in the individuals with schizophrenia.

We found that the schizophrenia group resided for a significantly longer proportion of the 8-min fMRI acquisition in states that were characterized by overall low activity in all networks, particularly low activation of the default mode and executive networks. This might explain the poor behavioral and emotional regulatory functions in schizophrenia (Breton et al., 2011; Orellana & Slachevsky, 2013), which contributes to increased negative symptoms (Strauss et al., 2013). Furthermore, states characterized by high activation of sensory networks were visited for a longer proportion of time, potentially corresponding to the sensory gating deficits in schizophrenia (de Wilde, Bour, Dingemans, Koelman, & Linszen, 2007; Patterson et al., 2008) leading to hallucinations (Bohlken, Hugdahl, & Sommer, 2017).

Figure 4 suggests that schizophrenia is associated with an inability to rapidly transition in and out of states with high DMN activation. This accords with the finding that the mean lifetimes of both DM*Hi*-Sen*Lo* and DM*Lo*-Sen*Hi* states were significantly higher in schizophrenia. Interestingly, while the schizophrenia group spent a significantly shorter *proportion of time* in the state characterized by an active DMN but inactive sensory networks (DM*Hi*-Sen*Lo*), the *duration of each activation* in this state was on average significantly longer (4–5 s) than the healthy comparison individuals. Thus, individuals with schizophrenia

do not often switch to this state compared to healthy subjects. This suggests that schizophrenia is associated with reduced dynamism of the DMN and that this network may be difficult to activate and deactivate in individuals with the disorder. In other words, while the DMN activates less frequently in schizophrenia, once it is activated, it remains active for abnormally long periods.

Therefore, the mechanisms that upregulate or downregulate DMN activation appears to be disrupted in schizophrenia. This deficit might explain the observed perseveration (Crider, 1997), particularly the impairments in set shifting (Ceaser et al., 2008). Given the role of the DMN in self-generated cognition and self-consciousness (Andrews-Hanna, 2012; Buckner, Andrews-Hanna, & Schacter, 2008; Raichle et al., 2001), this inability might also correspond to the disrupted sense of self (i.e., difficulty in differentiating self from others; Sass & Parnas, 2003; Wang, Metzak, & Woodward, 2011; Moe & Docherty, 2014) and "poor mental coordination" (Andreasen, Paradiso, & O'Leary, 1998) reported in schizophrenia. A number of task-based fMRI studies show that individuals with schizophrenia fail to deactivate the DMN (Anticevic, Repovs, & Barch, 2013; Calhoun, Maciejewski, Pearlson, & Kiehl, 2008; Camchong et al., 2011; Garrity et al., 2007; Hasenkamp, James, Boshoven, & Duncan, 2011; Kim et al., 2009; Pomarol-Clotet et al., 2008; Salgado-Pineda et al., 2011; Wang et al., 2011; Whitfield-Gabrieli et al., 2009). Studies have also reported a correspondence between the reduced task-related suppression in DMN and gray matter volume loss in some of the regions comprising this network (Pomarol-Clotet et al., 2010; Salgado-Pineda et al., 2011; Skudlarski et al., 2010; Zhou et al., 2008). In the present study, using a time-resolved approach,

we show that this inability to suppress DMN activity is evident even in the resting state.

Two of the states inferred—the DMLo-SenHi and DMHi-SenLo states, are characterized by an antagonistic relationship between default mode and sensory systems. While initial studies on RSNs report the existence of anticorrelation between these two systems (Fox et al., 2005; Greicius, Krasnow, Reiss, & Menon, 2003; Raichle et al., 2001), suggesting it to be a mechanism for "division of labor" between task-positive networks and DMN (Fransson, 2005, 2006) and an indicator of behavioral performance (Kelly, Uddin, Biswal, Castellanos, & Milham, 2008), later studies on connectivity dynamics have reported more complex relationships among RSNs (Allen et al., 2014; Chang & Glover, 2010; Hutchison et al., 2013b). In the current study, we observed instances of time when these two systems exhibit anticorrelated activity. This consisted of a state in which the DMN showing heightened activation and the other state with low DMN activity while sensory components in each case showing opposite trends. Notably, another study on dynamic functional network connectivity in schizophrenia also identified two such states (Rashid et al., 2014). Similarly, a state with reduced connectivity in DMN and hyperconnectivity in visual systems has been reported in healthy individuals with psychotic-like experiences (Barber, Lindquist, DeRosse, & Karlsgodt, 2018).

Interindividual variation in the severity of positive symptoms was significantly correlated with a multivariate combination consisting of the proportion of time spent across several states. More specifically, the severity of positive symptoms, as assessed with the SAPS, was associated with the following pattern of fractional occupancy times: *increased* occupancy of states characterized by an inactive default mode network (DMLo), inactive executive but active sensory networks (SenHi-ExLo), and overall low activity across all networks (Lo); together with *reduced* occupancy of the state characterized overall high activity across all networks (Hi). Both these relationships—the inverse association between severity of positive symptoms and DMN activation as well as the direct correspondence between positive symptoms and activation of sensory networks, are in agreement with previous task based (Menon, Anagnoson, Mathalon, Glover, & Pfefferbaum, 2001; Perlstein, Carter, Noll, & Cohen, 2001) and resting-state (Rotarska-Jagiela et al., 2010; Skudlarski et al., 2010) fMRI studies. Fractional occupancy times were not associated with cognitive deficits, durations of illness, antipsychotic medication dose, and measures of general functioning. While we hypothesized that altered transition dynamics may correlate with cognitive deficits, altered dynamics that specifically underpin cognition might only manifest during engagement of tasks, but not in the resting state considered in this study.

While there is strong evidence on lack of DMN suppression during goal-directed cognition in schizophrenia (Anticevic et al., 2012a; Calhoun et al., 2008; Camchong et al., 2011; Garrity et al., 2007; Hasenkamp et al., 2011; Kim et al., 2009; Pomarol-Clotet et al., 2008; Salgado-Pineda et al., 2011; Wang et al., 2011; Whitfield-Gabrieli et al., 2009), its exact causes remain unclear, fundamentally due to our limited understanding of the mechanisms underlying the functional antagonism between DMN and task-positive networks (Anticevic et al., 2012a). A few neuropharmacological studies have implicated defective synaptic mechanisms in psychotic conditions, mediated by

certain monoaminergics that prevent inhibitory interneuronal functions in the cortex (Anticevic et al., 2012b; Carhart-Harris et al., 2012; Dang, O'Neil, & Jagust, 2012; Minzenberg, Yoon, & Carter, 2011). This "cortical disinhibition" (Krystal et al., 2003) has been shown to affect the dynamic interplay between task-positive and task-negative systems, which was explained by plausible biophysical models based on conductance of different membrane receptors (Compte, Brunel, Goldman-Rakic, & Wang, 2000) and further validated by pharmacological experiments (Brunel & Wang, 2001; Krystal et al., 2003).

The singe-subject prediction analyses using fractional occupancy times as subject-specific features provided high classification accuracies (>80%) that remain consistent across different classifier models. This implies the utility of the model in capturing disease-related information, even when the states were estimated from the concatenated network time series. Previous studies on functional connectivity have reported accuracies in the range of 60–95% in classifying schizophrenia versus healthy subjects (Du, Zening, & Calhoun, 2018; Woo, Chang, Lindquist, & Wager, 2017); however, most of them employ ICA to define networks from the whole data, which leads to a bias in the cross validation. Using predefined maps for the delineation of RSNs, we could eliminate this drawback and by this way, the features become more comparable across subjects.

Intrascan head motion (Power, Barnes, Snyder, Schlaggar, & Petersen, 2012) is well-known to influence functional connectivity measures (Satterthwaite et al., 2012; Van Dijk, Sabuncu, & Buckner, 2012; Yendiki, Koldewyn, Kakunoori, Kanwisher, & Fischl, 2014), emphasizing the need for appropriate motion correction strategies, particularly in the case of time-resolved analyses (Laumann et al., 2016). At the same time, head motion has been shown to have a genetic basis (Couvy-Duchesne et al., 2014, 2016), rather than an artifact; and the choice of correction technique can potentially influence the specificity of imaging-based biomarkers (Parkes, Fulcher, Yücel, & Fornito, 2018; Zeng et al., 2014). In the case of modeling dynamics with the HMM, head motion can induce artificial state transitions, which confounds the summary measures calculated. However, as noted in Section 2.1, mean FD values were not significantly different between groups in our data. Furthermore, we repeated the between-group comparisons of fractional occupancy and mean lifetimes after regressing the mean FD values from each measure and performing inference on the resulting residuals. Supporting Information Figure S6 shows that between-group differences were unchanged when inference was performed on the residuals resulting from motion regression, suggesting that intrascan head motion did not significantly influence our findings.

Several limitations warrant consideration. First, the same reference maps were used to delineate RSNs in both the schizophrenia and healthy comparison groups, thereby disregarding any between-group differences in the spatial extent (Ma, Calhoun, Phlypo, & Adalı, 2014) of these networks. Second, fitting the HMM to the concatenated data yielded a single set of inferred states that represented a consensus across all individuals. While all individuals thus shared a common set of states, the amount of time spent in each state and the transition probabilities between states could vary between individuals. To improve the fit of the model, an alternative approach would have been to independently fit a separate HMM to each individual or each diagnostic category. However, this approach would

have substantially increased the model complexity and would not have allowed for state-specific statistics to be directly compared between groups. Third, the influence of intrascan head motion (Power et al., 2012) could have potentially confounded our observations. A standard motion correction algorithm was used in our analyses, but we have not adopted any stringent methods like scrubbing. However, there were no significant between-group differences in head motion in our subjects and our results remain significant even after regressing motion parameters from summary measures. The influence of antipsychotic medication (Moncrieff & Leo, 2010) on observed dynamics is also unknown. Finally, the effect of drowsiness or sleep (Deco et al., 2018; Tagliazucchi & Laufs, 2014) on our observations is unclear. Participants were instructed to remain awake during the scan, but there were no further measures to control or monitor sleep.

5 | CONCLUSION

The present study characterizes aberrant dynamic network interactions in schizophrenia. We observed that compared to a healthy comparison group, schizophrenia individuals spent greater amounts of time in states characterized by overall low activity, particularly within the DMN and executive networks. Interindividual variation in these attributes significantly correlated with the severity of positive symptoms, but not cognitive deficits, medication, and duration of illness. We also found that individuals with schizophrenia are not capable of regulating DMN activity as efficiently as healthy subjects, and as a result, have difficulty in activating and inactivating the DMN. We assessed the efficacy of different state occupancies as potential biomarkers for the disease using a machine learning classifier and observed that such models can achieve a high diagnostic accuracy. Further, we tested the reproducibility of the model on another data set and performed rigorous permutation testing to validate the robustness of model estimation.

ORCID

Akhil Kottaram 🆔 https://orcid.org/0000-0003-2446-2704
Luca Cocchi 🆔 https://orcid.org/0000-0003-3651-2676
Christos Pantelis 🆔 https://orcid.org/0000-0002-9565-0238

REFERENCES

Alexander-Bloch, A. F., Gogtay, N., Meunier, D., Birn, R., Clasen, L., Lalonde, F., ... Bullmore, E. T. (2010). Disrupted modularity and local connectivity of brain functional networks in childhood-onset schizophrenia. *Frontiers in Systems Neuroscience*, *4*, 147. https://doi.org/10.3389/fnsys.2010.00147

Allen, E. A., Damaraju, E., Plis, S. M., Erhardt, E. B., Eichele, T., Calhoun, V. D., et al. (2014). Tracking whole-brain connectivity dynamics in the resting state. *Cerebral Cortex*, *24*(3), 663–676. https://doi.org/10.1093/cercor/bhs352

Andreasen, N. C., Flaum, M., Arndt, S., Alliger, R., & Swayze, V. W. (1991). Positive and negative symptoms: Assessment and validity. In *Negative versus positive schizophrenia* (pp. 28–51). Berlin, Heidelberg: Springer Berlin Heidelberg. https://doi.org/10.1007/978-3-642-76841-5_3

Andreasen, N. C., Paradiso, S., & O'Leary, D. S. (1998). "Cognitive Dysmetria" as an integrative theory of schizophrenia: A dysfunction in cortical-subcortical-cerebellar circuitry? *Schizophrenia Bulletin*, *24*(2), 203–218.

Andrews-Hanna, J. R. (2012). The brain's default network and its adaptive role in internal mentation. *The Neuroscientist: A Review Journal Bringing Neurobiology, Neurology and Psychiatry*, *18*(3), 251–270. https://doi.org/10.1177/1073858411403316

Anticevic, A., Gancsos, M., Murray, J. D., Repovs, G., Driesen, N. R., Ennis, D. J., ... Corlett, P. R. (2012b). NMDA receptor function in large-scale Anticorrelated neural systems with implications for cognition and schizophrenia. *Proceedings of the National Academy of Sciences of the United States of America*, *109*(41), 16720–16725. https://doi.org/10.1073/pnas.1208494109

Anticevic, A., Cole, M. W., Murray, J. D., Corlett, P. R., Wang, X.-J., & Krystal, J. H. (2012a). The role of default network deactivation in cognition and disease. *Trends in Cognitive Sciences*, *16*(12), 584–592. https://doi.org/10.1016/j.tics.2012.10.008

Anticevic, A., Repovs, G., & Barch, D. M. (2013). Working memory encoding and maintenance deficits in schizophrenia: Neural evidence for activation and deactivation abnormalities. *Schizophrenia Bulletin*, *39*(1), 168–178. https://doi.org/10.1093/schbul/sbr107

Baker, A. P., Brookes, M. J., Rezek, I. A., Smith, S. M., Behrens, T., Smith, P. J. P., & Woolrich, M. (2014). Fast transient networks in

spontaneous human brain activity. *eLife*, *3*, e01867. https://doi.org/10.7554/eLife.01867

Barber, A. D., Lindquist, M. A., DeRosse, P., & Karlsgodt, K. H. (2018). Dynamic functional connectivity states reflecting psychotic-like experiences. *Biological Psychiatry: Cognitive Neuroscience and Neuroimaging*, *3*(5), 443–453. https://doi.org/10.1016/j.bpsc.2017.09.008

Bluhm, R. L., Miller, J., Lanius, R. A., Osuch, E. A., Boksman, K., Neufeld, R. W. J., ... Williamson, P. (2007). Spontaneous low-frequency fluctuations in the BOLD signal in schizophrenic patients: Anomalies in the default network. *Schizophrenia Bulletin*, *33*(4), 1004–1012. https://doi.org/10.1093/schbul/sbm052

Bluhm, R. L., Miller, J., Lanius, R. A., Osuch, E. A., Boksman, K., Neufeld, R. W. J., ... Williamson, P. C. (2009). Retrosplenial cortex connectivity in schizophrenia. *Psychiatry Research: Neuroimaging*, *174*(1), 17–23. https://doi.org/10.1016/j.pscychresns.2009.03.010

Bohlken, M. M., Hugdahl, K., & Sommer, I. E. C. (2017). Auditory verbal hallucinations: Neuroimaging and treatment. *Psychological Medicine*, *47*(02), 199–208. https://doi.org/10.1017/S003329171600115X

Bora, E., & Pantelis, C. (2015). Meta-analysis of cognitive impairment in first-episode bipolar disorder: Comparison with first-episode schizophrenia and healthy controls. *Schizophrenia Bulletin*, *41*(5), 1095–1104. https://doi.org/10.1093/schbul/sbu198

Breakspear, M., Terry, J. R., Friston, K. J., Harris, A. W. F., Williams, L. M., Brown, K., ... Gordon, E. (2003). A disturbance of nonlinear interdependence in scalp EEG of subjects with first episode schizophrenia. *NeuroImage*, *20*(1), 466–478. https://doi.org/10.1016/S1053-8119(03)00332-X

Bressler, S. L., & Menon, V. (2010). Large-scale brain networks in cognition: Emerging methods and principles. *Trends in Cognitive Sciences*, *14*(6), 277–290. https://doi.org/10.1016/j.tics.2010.04.004

Breton, F., Planté, A., Legauffre, C., Morel, N., Adès, J., Gorwood, P., ... Dubertret, C. (2011). The executive control of attention differentiates patients with schizophrenia, their first-degree relatives and healthy controls. *Neuropsychologia*, *49*(2), 203–208. https://doi.org/10.1016/j.neuropsychologia.2010.11.019

Brunel, N., & Wang, X.-J. (2001). Effects of neuromodulation in a cortical network model of object working memory dominated by recurrent inhibition. *Journal of Computational Neuroscience*, *11*(1), 63–85. https://doi.org/10.1023/A:1011204814320

Buckner, R. L., Andrews-Hanna, J. R., & Schacter, D. L. (2008). The brain's default network. *Annals of the New York Academy of Sciences*, *1124*(1), 1–38. https://doi.org/10.1196/annals.1440.011

Cabral, J., Kringelbach, M. L., & Deco, G. (2014). Exploring the network dynamics underlying brain activity during rest. *Progress in Neurobiology*, *114*, 102–131. https://doi.org/10.1016/j.pneurobio.2013.12.005

Cabral, J., Kringelbach, M. L., & Deco, G. (2017). Functional connectivity dynamically evolves on multiple time-scales over a static structural connectome: Models and mechanisms. *NeuroImage*, *160*, 84–96. https://doi.org/10.1016/J.NEUROIMAGE.2017.03.045

Cabral, J., Vidaurre, D., Marques, P., Magalhães, R., Moreira, P. S., Soares, J. M., ... Kringelbach, M. L. (2017). Cognitive performance in healthy older adults relates to spontaneous switching between states of functional connectivity during rest. *Scientific Reports*, *7*(1), 5135. https://doi.org/10.1038/s41598-017-05425-7

Calhoun, V. D., Eichele, T., & Pearlson, G. (2009). Functional brain networks in schizophrenia: A review. *Frontiers in Human Neuroscience*, *3*, 17. https://doi.org/10.3389/neuro.09.017.2009

Calhoun, V. D., Maciejewski, P. K., Pearlson, G. D., & Kiehl, K. A. (2008). Temporal lobe and 'default' hemodynamic brain modes discriminate between schizophrenia and bipolar disorder. *Human Brain Mapping*, *29*(11), 1265–1275. https://doi.org/10.1002/hbm.20463

Calhoun, V. D., Miller, R., Pearlson, G., & Adalı, T. (2014). The chronnectome: Time-varying connectivity networks as the next frontier in FMRI data discovery. *Neuron*, *84*(2), 262–274. https://doi.org/10.1016/j.neuron.2014.10.015

Calhoun, V. D., Sui, J., Kiehl, K., Turner, J., Allen, E., & Pearlson, G. (2012). Exploring the psychosis functional connectome: Aberrant intrinsic networks in schizophrenia and bipolar disorder. *Frontiers in Psychiatry*, *2*, 75. https://doi.org/10.3389/fpsyt.2011.00075

Camchong, J., MacDonald, A. W., Bell, C., Mueller, B. A., Lim, K. O., & Lim, K. O. (2011). Altered functional and anatomical connectivity in schizophrenia. *Schizophrenia Bulletin*, *37*(3), 640–650. https://doi.org/10.1093/schbul/sbp131

Carhart-Harris, R. L., Erritzoe, D., Williams, T., Stone, J. M., Reed, L. J., Colasanti, A., et al. (2012). Neural correlates of the psychedelic state as determined by FMRI studies with psilocybin, *109*(6), 2138–2143. https://doi.org/10.1073/pnas.1119598109

Ceaser, A. E., Goldberg, T. E., Egan, M. F., McMahon, R. P., Weinberger, D. R., & Gold, J. M. (2008). Set-shifting ability and schizophrenia: A marker of clinical illness or an intermediate phenotype? *Biological Psychiatry*, *64*(9), 782–788. https://doi.org/10.1016/j.biopsych.2008.05.009

Chang, C., & Glover, G. H. (2010). Time–frequency dynamics of resting-state brain connectivity measured with FMRI. *NeuroImage*, *50*(1), 81–98. https://doi.org/10.1016/j.neuroimage.2009.12.011

Cocchi, L., Halford, G. S., Zalesky, A., Harding, I. H., Ramm, B. J., Cutmore, T., ... Mattingley, J. B. (2014). Complexity in relational processing predicts changes in functional brain network dynamics. *Cerebral Cortex*, *24*(9), 2283–2296. https://doi.org/10.1093/cercor/bht075

Cocchi, L., Harding, I. H., Lord, A., Pantelis, C., Yucel, M., & Zalesky, A. (2014). Disruption of structure–function coupling in the schizophrenia connectome. *NeuroImage: Clinical*, *4*, 779–787. https://doi.org/10.1016/j.nicl.2014.05.004

Cocchi, L., Zalesky, A., Fornito, A., & Mattingley, J. B. (2013). Dynamic cooperation and competition between brain systems during cognitive control. *Trends in Cognitive Sciences*, *17*(10), 493–501. https://doi.org/10.1016/J.TICS.2013.08.006

Cole, M. W., Ito, T., Bassett, D. S., & Schultz, D. H. (2016). Activity flow over resting-state networks shapes cognitive task activations. *Nature Neuroscience*, *19*(12), 1718–1726. https://doi.org/10.1038/nn.4406

Compte, A., Brunel, N., Goldman-Rakic, P. S., & Wang, X.-J. (2000). Synaptic mechanisms and network dynamics underlying spatial working memory in a cortical network model. *Cerebral Cortex*, *10*(9), 910–923. https://doi.org/10.1093/cercor/10.9.910

Cordes, D., Haughton, V. M., Arfanakis, K., Carew, J. D., Turski, P. A., Moritz, C. H., ... Meyerand, M. E. (2001). Frequencies contributing to functional connectivity in the cerebral cortex in "resting-state" data. *American Journal of Neuroradiology*, *22*(7), 1326–1333 Retrieved from http://www.ncbi.nlm.nih.gov/pubmed/11498421

Couvy-Duchesne, B., Blokland, G. A., Hickie, I. B., Thompson, P. M., Martin, N. G., de Zubicaray, G. I., ... Wright, M. J. (2014). Heritability of head motion during resting state functional MRI in 462 healthy twins. *NeuroImage*, *102*, 424–434.

Couvy-Duchesne, B., Ebejer, J. L., Gillespie, N. A., Duffy, D. L., Hickie, I. B., Thompson, P. M., ... Wright, M. J. (2016). Head motion and inattention/hyperactivity share common genetic influences: Implications for fMRI studies of ADHD. *PLoS One*, *11*(1), e0146271.

Crider, A. (1997). Perseveration in schizophrenia. *Schizophrenia Bulletin*, *23*(1), 63–74 Retrieved from http://www.ncbi.nlm.nih.gov/pubmed/9050113

Damaraju, E., Allen, E. A., Belger, A., Ford, J. M., McEwen, S., Mathalon, D. H., et al. (2014). Dynamic functional connectivity analysis reveals transient states of dysconnectivity in schizophrenia. *NeuroImage: Clinical*, *5*, 298–308. https://doi.org/10.1016/j.nicl.2014.07.003

Dang, L. C., O'Neil, J. P., & Jagust, W. J. (2012). Dopamine supports coupling of attention-related networks. *The Journal of Neuroscience*, *32*(28), 9582–9587. https://doi.org/10.1523/JNEUROSCI.0909-12.2012

de Wilde, O. M., Bour, L. J., Dingemans, P. M., Koelman, J. H. T. M., & Linszen, D. H. (2007). A meta-analysis of P50 studies in patients with schizophrenia and relatives: Differences in methodology between research groups. *Schizophrenia Research*, *97*(1–3), 137–151. https://doi.org/10.1016/j.schres.2007.04.028

Deco, G., Cabral, J., Saenger, V. M., Boly, M., Tagliazucchi, E., Laufs, H., ... Kringelbach, M. L. (2018). Perturbation of whole-brain dynamics in silico reveals mechanistic differences between brain states. *NeuroImage*, *169*, 46–56. https://doi.org/10.1016/j.neuroimage.2017.12.009

Deco, G., & Jirsa, V. K. (2012). Ongoing cortical activity at rest: Criticality, multistability, and ghost attractors. *Journal of Neuroscience*, *32*(10, 10.1523/JNEUROSCI.2523-11.2012), 3366–3375.

Deco, G., Jirsa, V. K., & McIntosh, A. R. (2011). Emerging concepts for the dynamical organization of resting-state activity in the brain. *Nature Reviews Neuroscience*, *12*(1), 43–56. https://doi.org/10.1038/nrn2961

Du, Y., Zening, F., & Calhoun, V. D. (2018). Classification and prediction of brain disorders using functional connectivity: Promising but challenging. *Frontiers in Neuroscience*, 12, 525. https://doi.org/10.3389/fnins.2018.00525

Elvevåg, B., & Goldberg, T. E. (2000). Cognitive impairment in schizophrenia is the core of the disorder. *Critical Reviews in Neurobiology*, 14(1), 1, 21 Retrieved from http://www.ncbi.nlm.nih.gov/pubmed/11253953

Fornito, A., Yoon, J., Zalesky, A., Bullmore, E. T., & Carter, C. S. (2011). General and specific functional connectivity disturbances in first-episode schizophrenia during cognitive control performance. *Biological Psychiatry*, 70(1), 64–72. https://doi.org/10.1016/j.biopsych.2011.02.019

Fornito, A., Zalesky, A., Pantelis, C., & Bullmore, E. T. (2012). Schizophrenia, neuroimaging and connectomics. *NeuroImage*, 62(4), 2296–2314. https://doi.org/10.1016/j.neuroimage.2011.12.090

Fox, M. D., & Greicius, M. (2010). Clinical applications of resting state functional connectivity. *Frontiers in Systems Neuroscience*, 4, 19. https://doi.org/10.3389/fnsys.2010.00019

Fox, M. D., Snyder, A. Z., Vincent, J. L., Corbetta, M., Van Essen, D. C., & Raichle, M. E. (2005). From the cover: The human brain is intrinsically organized into dynamic, anticorrelated functional networks. *Proceedings of the National Academy of Sciences of the United States of America*, 102(27), 9673–9678. https://doi.org/10.1073/pnas.0504136102

Fransson, P. (2005). Spontaneous low-frequency BOLD signal fluctuations: An FMRI investigation of the resting-state default mode of brain function hypothesis. *Human Brain Mapping*, 26(1), 15–29. https://doi.org/10.1002/hbm.20113

Fransson, P. (2006). How default is the default mode of brain function? *Neuropsychologia*, 44(14), 2836–2845. https://doi.org/10.1016/j.neuropsychologia.2006.06.017

Friston, K. J., Williams, S., Howard, R., Frackowiak, R. S. J., & Turner, R. (1996). Movement-related effects in FMRI time-series. *Magnetic Resonance in Medicine*, 35(3), 346–355. https://doi.org/10.1002/mrm.1910350312

Fu, Z., Yiheng, T., Di, X., Yuhui, D., Pearlson, G. D., Turner, J. A., … Calhoun, V. D. (2017). Characterizing dynamic amplitude of low-frequency fluctuation and its relationship with dynamic functional connectivity: An application to schizophrenia. *NeuroImage*, 180, 619–631. https://doi.org/10.1016/J.NEUROIMAGE.2017.09.035

Garrity, A. G., Pearlson, G. D., McKiernan, K., Lloyd, D., Kiehl, K. A., & Calhoun, V. D. (2007). Aberrant 'default mode' functional connectivity in schizophrenia. *American Journal of Psychiatry*, 164(3), 450–457. https://doi.org/10.1176/ajp.2007.164.3.450

Goldman, H. H., Skodol, A. E., & Lave, T. R. (1992). Revising Axis V for DSM-IV: A review of measures of social functioning. *American Journal of Psychiatry*, 149(9), 1148–1156. https://doi.org/10.1176/ajp.149.9.1148

Greicius, M. D., Krasnow, B., Reiss, A. L., & Menon, V. (2003). Functional connectivity in the resting brain: A network analysis of the default mode hypothesis. *Proceedings of the National Academy of Sciences of the United States of America*, 100(1), 253–258. https://doi.org/10.1073/PNAS.0135058100

Gur, R. E., McGrath, C., Chan, R. M., Schroeder, L., Turner, T., Turetsky, B. I., … Gur, R. C. (2002). An FMRI study of facial emotion processing in patients with schizophrenia. *American Journal of Psychiatry*, 159(12), 1992–1999. https://doi.org/10.1176/appi.ajp.159.12.1992

Gur, R. E., & Gur, R. C. (2010). Functional magnetic resonance imaging in schizophrenia. *Dialogues in Clinical Neuroscience*, 12(3), 333–343 Retrieved from http://www.ncbi.nlm.nih.gov/pubmed/20954429

Hall, R. C., & Parks, J. (1995). The modified global assessment of functioning scale: Addendum. *Psychosomatics*, 36(4), 416–417. https://doi.org/10.1016/S0033-3182(95)71656-5

Harrison, B. J., Yücel, M., Pujol, J., & Pantelis, C. (2007). Task-induced deactivation of midline cortical regions in schizophrenia assessed with FMRI. *Schizophrenia Research*, 91(1–3), 82–86. https://doi.org/10.1016/J.SCHRES.2006.12.027

Hasenkamp, W., James, G. A., Boshoven, W., & Duncan, E. (2011). Altered engagement of attention and default networks during target detection in schizophrenia. *Schizophrenia Research*, 125(2–3), 169–173. https://doi.org/10.1016/j.schres.2010.08.041

Hindriks, R., Adhikari, M. H., Murayama, Y., Ganzetti, M., Mantini, D., Logothetis, N. K., & Deco, G. (2016). Can sliding-window correlations reveal dynamic functional connectivity in resting-state FMRI? *NeuroImage*, 127, 242–256. https://doi.org/10.1016/j.neuroimage.2015.11.055

Hugdahl, K., Rund, B. R., Lund, A., Asbjørnsen, A., Egeland, J., Ersland, L., … Thomsen, T. (2004). Brain activation measured with FMRI during a mental arithmetic task in schizophrenia and major depression. *American Journal of Psychiatry*, 161(2), 286–293. https://doi.org/10.1176/appi.ajp.161.2.286

Hutchison, R. M., Womelsdorf, T., Allen, E. A., Bandettini, P. A., Calhoun, V. D., Corbetta, M., et al. (2013a). Dynamic functional connectivity: Promise, issues, and interpretations. *NeuroImage*, 80, 360–378. https://doi.org/10.1016/j.neuroimage.2013.05.079

Hutchison, R. M., Womelsdorf, T., Gati, J. S., Everling, S., & Menon, R. S. (2013b). Resting-state networks show dynamic functional connectivity in awake humans and anesthetized macaques. *Human Brain Mapping*, 34(9), 2154–2177. https://doi.org/10.1002/hbm.22058

Jafri, M. J., Pearlson, G. D., Stevens, M., & Calhoun, V. D. (2008). A method for functional network connectivity among spatially independent resting-state components in schizophrenia. *NeuroImage*, 39(4), 1666–1681. https://doi.org/10.1016/J.NEUROIMAGE.2007.11.001

Kelly, A. M. C., Uddin, L. Q., Biswal, B. B., Castellanos, F. X., & Milham, M. P. (2008). Competition between functional brain networks mediates behavioral variability. *NeuroImage*, 39(1), 527–537. https://doi.org/10.1016/j.neuroimage.2007.08.008

Kim, D. I. L., Manoach, D. S., Mathalon, D. H., Turner, J. A., Mannell, M., Brown, G. G., et al. (2009). Dysregulation of working memory and default-mode networks in schizophrenia using independent component analysis, an FBIRN and MCIC study. *Human Brain Mapping*, 30(11), 3795–3811. https://doi.org/10.1002/hbm.20807

Kircher, T. T. J., & Thienel, R. (2005). Functional brain imaging of symptoms and cognition in schizophrenia. *Progress in Brain Research*, 150, 299–604. https://doi.org/10.1016/S0079-6123(05)50022-0

Kottaram, A., Johnston, L., Ganella, E., Pantelis, C., Kotagiri, R., & Zalesky, A. (2018). Spatio-temporal dynamics of resting-state brain networks improve single-subject prediction of schizophrenia diagnosis. *Human Brain Mapping*, 39, 3663–3681. https://doi.org/10.1002/hbm.24202

Krystal, J. H., Cyril D'Souza, D., Mathalon, D., Perry, E., Belger, A., & Hoffman, R. (2003). NMDA receptor antagonist effects, cortical glutamatergic function, and schizophrenia: Toward a paradigm shift in medication development. *Psychopharmacology*, 169(3–4), 215–233. https://doi.org/10.1007/s00213-003-1582-z

Laumann, T. O., Snyder, A. Z., Mitra, A., Gordon, E. M., Gratton, C., Adeyemo, B., … McCarthy, J. E. (2016). On the stability of BOLD fMRI correlations. *Cerebral Cortex*, 27(10), 4719–4732.

Leonardi, N., & Van De Ville, D. (2015). On spurious and real fluctuations of dynamic functional connectivity during rest. *NeuroImage*, 104, 430–436. https://doi.org/10.1016/j.neuroimage.2014.09.007

Liang, M., Zhou, Y., Jiang, T., Liu, Z., Tian, L., Liu, H., & Hao, Y. (2006). Widespread functional disconnectivity in schizophrenia with resting-state functional magnetic resonance imaging. *Neuroreport*, 17(2), 209–213 Retrieved from http://www.ncbi.nlm.nih.gov/pubmed/16407773

Liegeois, R., Laumann, T. O., Snyder, A. Z., Zhou, H. J., & Thomas Yeo, B. T. (2017). Interpreting temporal fluctuations in resting-state functional connectivity MRI. *Neuroimage*, 163, 437–455. Retrieved from https://doi.org/10.1016/j.neuroimage.2017.09.012

Lindquist, M. A., Xu, Y., Nebel, M. B., & Caffo, B. S. (2014). Evaluating dynamic bivariate correlations in resting-state FMRI: A comparison study and a new approach. *NeuroImage*, 101, 531–546. https://doi.org/10.1016/j.neuroimage.2014.06.052

Liu, H., Liu, Z., Liang, M., Hao, Y., Tan, L., Kuang, F., … Jiang, T. (2006). Decreased regional homogeneity in schizophrenia: A resting state functional magnetic resonance imaging study. *Neuroreport*, 17(1), 19–22 Retrieved from http://www.ncbi.nlm.nih.gov/pubmed/16361943

Liu, Y., Liang, M., Zhou, Y., He, Y., Hao, Y., Song, M., … Jiang, T. (2008). Disrupted small-world networks in schizophrenia. *Brain*, 131(4), 945–961. https://doi.org/10.1093/brain/awn018

Ma, S., Calhoun, V. D., Phlypo, R., & Adalı, T. (2014). Dynamic changes of spatial functional network connectivity in healthy individuals and schizophrenia patients using independent vector analysis. *NeuroImage*, 90, 196–206. https://doi.org/10.1016/j.neuroimage.2013.12.063

Manoach, D. S., Press, D. Z., Thangaraj, V., Searl, M. M., Goff, D. C., Halpern, E., … Warach, S. (1999). Schizophrenic subjects activate

dorsolateral prefrontal cortex during a working memory task, as measured by FMRI. *Biological Psychiatry*, 45(9), 1128–1137. https://doi.org/10.1016/S0006-3223(98)00318-7

Menon, V., Anagnoson, R. T., Mathalon, D. H., Glover, G. H., & Pfefferbaum, A. (2001). Functional neuroanatomy of auditory working memory in schizophrenia: Relation to positive and negative symptoms. https://doi.org/10.1006/nimg.2000.0699.

Miller, R. L., Yaesoubi, M., Turner, J. A., Mathalon, D., Preda, A., Pearlson, G., ... Calhoun, V. D. (2016). Higher dimensional meta-state analysis reveals reduced resting FMRI connectivity dynamism in schizophrenia patients. *PLoS One*, 11(3), e0149849. https://doi.org/10.1371/journal.pone.0149849

Minzenberg, M. J., Yoon, J. H., & Carter, C. S. (2011). Modafinil modulation of the default mode network. *Psychopharmacology*, 215(1), 23–31. https://doi.org/10.1007/s00213-010-2111-5

Moe, A. M., & Docherty, N. M. (2014). Schizophrenia and the sense of self. *Schizophrenia Bulletin*, 40(1), 161–168. https://doi.org/10.1093/schbul/sbt121

Moncrieff, J., & Leo, J. (2010). A systematic review of the effects of antipsychotic drugs on brain volume. *Psychological Medicine*, 40(9), 1409–1422. https://doi.org/10.1017/S0033291709992297

Murphy, K., Birn, R. M., Handwerker, D. A., Jones, T. B., & Bandettini, P. A. (2009). The impact of global signal regression on resting state correlations: Are anti-correlated networks introduced? *NeuroImage*, 44(3), 893–905. https://doi.org/10.1016/j.neuroimage.2008.09.036

Orellana, G., & Slachevsky, A. (2013). Executive functioning in schizophrenia. *Frontiers in Psychiatry*, 4, 35. https://doi.org/10.3389/fpsyt.2013.00035

Ou, J., Xie, L., Jin, C., Li, X., Zhu, D., Jiang, R., ... Liu, T. (2015). Characterizing and differentiating brain state dynamics via hidden Markov models. *Brain Topography*, 28(5), 666–679. https://doi.org/10.1007/s10548-014-0406-2

Parkes, L., Fulcher, B., Yücel, M., & Fornito, A. (2018). An evaluation of the efficacy, reliability, and sensitivity of motion correction strategies for resting-state functional MRI. *NeuroImage*, 171, 415–436.

Patterson, J. V., Hetrick, W. P., Boutros, N. N., Yi, J., Sandman, C., Stern, H., ... Bunney, W. E. (2008). P50 sensory gating ratios in schizophrenics and controls: A review and data analysis. *Psychiatry Research*, 158(2), 226–247. https://doi.org/10.1016/j.psychres.2007.02.009

Perlstein, W. M., Carter, C. S., Noll, D. C., & Cohen, J. D. (2001). Relation of prefrontal cortex dysfunction to working memory and symptoms in schizophrenia. *American Journal of Psychiatry*, 158(7), 1105–1113. https://doi.org/10.1176/appi.ajp.158.7.1105

Pomarol-Clotet, E., Canales-Rodríguez, E. J., Salvador, R., Sarró, S., Gomar, J. J., Vila, F., ... McKenna, P. J. (2010). Medial prefrontal cortex pathology in schizophrenia as revealed by convergent findings from multimodal imaging. *Molecular Psychiatry*, 15(8), 823–830. https://doi.org/10.1038/mp.2009.146

Pomarol-Clotet, E., Salvador, R., Sarró, S., Gomar, J., Vila, F., Martínez, Á., ... McKenna, P. J. (2008). Failure to deactivate in the prefrontal cortex in schizophrenia: Dysfunction of the default mode network? *Psychological Medicine*, 38(8), 1185–1193. https://doi.org/10.1017/S0033291708003565

Power, J. D., Barnes, K. A., Snyder, A. Z., Schlaggar, B. L., & Petersen, S. E. (2012). Spurious but systematic correlations in functional connectivity MRI networks arise from subject motion. *NeuroImage*, 59(3), 2142–2154. https://doi.org/10.1016/j.neuroimage.2011.10.018

Preti, M. G., Bolton, T. A. W., & Van De Ville, D. (2016). The dynamic functional connectome: State-of-the-art and perspectives. *NeuroImage*, 160, 41–54. https://doi.org/10.1016/j.neuroimage.2016.12.061

Quinn, A. J., Vidaurre, D., Abeysuriya, R., Becker, R., Nobre, A. C., & Woolrich, M. W. (2018). Task-evoked dynamic network analysis through hidden Markov modeling, 12, 603. *Frontiers in Neuroscience*, 12.

Raichle, M. E., MacLeod, A. M., Snyder, A. Z., Powers, W. J., Gusnard, D. A., & Shulman, G. L. (2001). A default mode of brain function. *Proceedings of the National Academy of Sciences of the United States of America*, 98(2), 676–682. https://doi.org/10.1073/pnas.98.2.676

Rashid, B., Damaraju, E., Pearlson, G. D., Calhoun, V. D., Koch, G., & Diwadkar, V. A. (2014). Dynamic connectivity states estimated from resting FMRI identify differences among schizophrenia, bipolar

disorder, and healthy control subjects. https://doi.org/10.3389/fnhum.2014.00897.

Rezek, I., & Roberts, S. (2005). Ensemble hidden Markov models with extended observation densities for biosignal analysis. In *Probabilistic modeling in bioinformatics and medical informatics* (pp. 419–450). London: Springer-Verlag. Accessed August 24, 2016. doi:10.1007/1-84628-119-9_14

Rotarska-Jagiela, A., van de Ven, V., Oertel-Knöchel, V., Uhlhaas, P. J., Vogeley, K., & Linden, D. E. J. (2010). Resting-state functional network correlates of psychotic symptoms in schizophrenia. *Schizophrenia Research*, 117(1), 21–30. https://doi.org/10.1016/J.SCHRES.2010.01.001

Rubinov, M., Knock, S. A., Stam, C. J., Micheloyannis, S., Harris, A. W. F., Williams, L. M., & Breakspear, M. (2009). Small-world properties of nonlinear brain activity in schizophrenia. *Human Brain Mapping*, 30(2), 403–416. https://doi.org/10.1002/hbm.20517

Ryali, S., Supekar, K., Chen, T., Kochalka, J., Cai, W., Nicholas, J., ... Menon, V. (2016). Temporal dynamics and developmental maturation of salience, default and central-executive network interactions revealed by Variational Bayes hidden Markov modeling. *PLoS Computational Biology*, 12(12), e1005138. https://doi.org/10.1371/journal.pcbi.1005138

Sahakian, B. J., Morris, R. G., Evenden, J. L., Heald, A., Levy, R., Philpot, M., & Robbins, T. W. (1988). A comparative study of visuospatial memory and learning in Alzheimer-type dementia and Parkinson's disease. *Brain: A Journal of Neurology*, 111(Pt 3), 695–718 Retrieved from http://www.ncbi.nlm.nih.gov/pubmed/3382917

Salgado-Pineda, P., Fakra, E., Delaveau, P., McKenna, P. J., Pomarol-Clotet, E., & Blin, O. (2011). Correlated structural and functional brain abnormalities in the default mode network in schizophrenia patients. *Schizophrenia Research*, 125(2–3), 101–109. https://doi.org/10.1016/j.schres.2010.10.027

Salvador, R., Martínez, A., Pomarol-Clotet, E., Sarró, S., Suckling, J., & Bullmore, E. (2007). Frequency based mutual information measures between clusters of brain regions in functional magnetic resonance imaging. *NeuroImage*, 35(1), 83–88. https://doi.org/10.1016/j.neuroimage.2006.12.001

Sass, L. A., & Parnas, J. (2003). Schizophrenia, consciousness, and the self. *Schizophrenia Bulletin*, 29(3), 427–444 Retrieved from http://www.ncbi.nlm.nih.gov/pubmed/14609238

Satterthwaite, T. D., Wolf, D. H., Loughead, J., Ruparel, K., Elliott, M. A., Hakonarson, H., ... Gur, R. E. (2012). Impact of in-scanner head motion on multiple measures of functional connectivity: Relevance for studies of neurodevelopment in youth. *NeuroImage*, 60(1), 623–632.

Sheehan, D. V., Lecrubier, Y., Sheehan, K. H., Amorim, P., Janavs, J., Weiller, E., ... Dunbar, G. C. (1998). The mini-international neuropsychiatric interview (M.I.N.I.): The development and validation of a structured diagnostic psychiatric interview for DSM-IV and ICD-10. *The Journal of Clinical Psychiatry*, 59(Suppl. 20), 22–33; quiz 34–57 Retrieved from http://www.ncbi.nlm.nih.gov/pubmed/9881538

Shirer, W. R., Ryali, S., Rykhlevskaia, E., Menon, V., & Greicius, M. D. (2012). Decoding subject-driven cognitive states with whole-brain connectivity patterns. *Cerebral Cortex*, 22(1), 158–165. https://doi.org/10.1093/cercor/bhr099

Skudlarski, P., Jagannathan, K., Anderson, K., Stevens, M. C., Calhoun, V. D., Skudlarska, B. A., & Pearlson, G. (2010). Brain connectivity is not only lower but different in schizophrenia: A combined anatomical and functional approach. *Biological Psychiatry*, 68(1), 61–69. https://doi.org/10.1016/j.biopsych.2010.03.035

Smith, S. M., Beckmann, C. F., Andersson, J., Auerbach, E. J., Bijsterbosch, J., Douaud, G., ... WU-Minn HCP Consortium. (2013). Resting-state FMRI in the human connectome project. *NeuroImage*, 80, 144–168. https://doi.org/10.1016/ j.neuroimage.2013.05.039

Sporns, O. (2013). Structure and function of complex brain networks. *Dialogues in Clinical Neuroscience*, 15(3), 247–262 Retrieved from http://www.ncbi.nlm.nih.gov/pubmed/24174898

Strauss, G. P., Kappenman, E. S., Culbreth, A. J., Catalano, L. T., Lee, B. G., & Gold, J. M. (2013). Emotion regulation abnormalities in schizophrenia: Cognitive change strategies fail to decrease the neural response to unpleasant stimuli. *Schizophrenia Bulletin*, 39(4), 872–883. https://doi.org/10.1093/schbul/sbs186

Su, J., Shen, H., Zeng, L.-L., Qin, J., Liu, Z., & Hu, D. (2016). Heredity characteristics of schizophrenia shown by dynamic functional connectivity analysis of resting-state functional MRI scans of unaffected siblings. *Neuroreport*, *27*(11), 843–848. https://doi.org/10.1097/WNR. 0000000000000622

Taghia, J., Cai, W., Ryali, S., Kochalka, J., Nicholas, J., Chen, T., & Menon, V. (2018). Uncovering hidden brain state dynamics that regulate performance and decision-making during cognition. *Nature Communications*, *9*(1), 2505. https://doi.org/10.1038/s41467-018-04723-6

Tagliazucchi, E., & Laufs, H. (2014). Decoding wakefulness levels from typical FMRI resting-state data reveals reliable drifts between wakefulness and sleep. *Neuron*, *82*(3), 695–708. https://doi.org/10.1016/j.neuron. 2014.03.020

van den Heuvel, M. P., & Fornito, A. (2014). Brain networks in schizophrenia. *Neuropsychology Review*, *24*(1), 32–48. https://doi.org/10.1007/ s11065-014-9248-7

Van Dijk, K. R., Sabuncu, M. R., & Buckner, R. L. (2012). The influence of head motion on intrinsic functional connectivity MRI. *NeuroImage*, *59*(1), 431–438.

Van Essen, D. C., Smith, S. M., Barch, D. M., Behrens, T. E. J., Yacoub, E., Ugurbil, K., & for the WU-Minn HCP WU-Minn HCP Consortium. (2013). The WU-Minn human connectome project: An overview. *NeuroImage*, *80*, 62–79. https://doi.org/10.1016/j.neuroimage.2013.05.041

Vidaurre, D., Quinn, A. J., Baker, A. P., Dupret, D., Tejero-Cantero, A., & Woolrich, M. W. (2016). Spectrally resolved fast transient brain states in electrophysiological data. *NeuroImage*, *126*, 81–95. https://doi. org/10.1016/J.NEUROIMAGE.2015.11.047

Vidaurre, D., Smith, S. M., & Woolrich, M. W. (2017a). Brain network dynamics are hierarchically organized in time. *Proceedings of the National Academy of Sciences of the United States of America*, *114*(48), 12827–12832. https://doi.org/10.1073/pnas.1705120114

Vidaurre, D., Abeysuriya, R., Becker, R., Quinn, A. J., Alfaro-Almagro, F., Smith, S. M., & Woolrich, M. W. (2017b). Discovering dynamic brain networks from big data in rest and task. *NeuroImage*, *180*, 646–656. https://doi.org/10.1016/J.NEUROIMAGE.2017.06.077

Wang, L., Metzak, P. D., & Woodward, T. S. (2011). Aberrant connectivity during self-other source monitoring in schizophrenia. *Schizophrenia Research*, *125*(2–3), 136–142. https://doi.org/10.1016/j.schres.2010. 11.012

Wechsler, D. (1955). *Manual for the Wechsler adult intelligence scale*. http:// psycnet.apa.org/record/1955-07334-000

Whitfield-Gabrieli, S., Thermenos, H. W., Milanovic, S., Tsuang, M. T., Faraone, S. V., McCarley, R. W., ... Seidman, L. J. (2009). Hyperactivity and hyperconnectivity of the default network in schizophrenia and in first-degree relatives of persons with schizophrenia. *Proceedings of the National Academy of Sciences*, *106*(4), 1279–1284. https://doi.org/10. 1073/pnas.0809141106

Woo, C.-W., Chang, L. J., Lindquist, M. A., & Wager, T. D. (2017). Building better biomarkers: Brain models in translational neuroimaging. *Nature Neuroscience*, *20*(3), 365–377. https://doi.org/10.1038/nn.4478

Xu, H., Jianpo, S., Qin, J., Li, M., Zeng, L.-L., Hu, D., & Shen, H. (2018). Impact of global signal regression on characterizing dynamic functional connectivity and brain states. *NeuroImage*, *173*, 127–145. https://doi. org/10.1016/J.NEUROIMAGE.2018.02.036

Yendiki, A., Koldewyn, K., Kakunoori, S., Kanwisher, N., & Fischl, B. (2014). Spurious group differences due to head motion in a diffusion MRI study. *NeuroImage*, *88*, 79–90.

Yoon, J. H., Minzenberg, M. J., Ursu, S., Walters, R., Wendelken, C., Daniel Ragland, J., & Carter, C. S. (2008). Association of dorsolateral prefrontal cortex dysfunction with disrupted coordinated brain activity in schizophrenia: Relationship with impaired cognition, behavioral disorganization, and global function. *American Journal of Psychiatry*, *165*(8), 1006–1014. https://doi.org/10.1176/appi.ajp.2008.07060945

Zalesky, A., & Breakspear, M. (2015). Towards a statistical test for functional connectivity dynamics. *NeuroImage*, *114*, 466–470. https://doi. org/10.1016/j.neuroimage.2015.03.047

Zalesky, A., Fornito, A., & Bullmore, E. T. (2010). Network-based statistic: Identifying differences in brain networks. *NeuroImage*, *53*(4), 1197–1207.

Zeng, L. L., Wang, D., Fox, M. D., Sabuncu, M., Hu, D., Ge, M., ... Liu, H. (2014). Neurobiological basis of head motion in brain imaging. *Proceedings of the National Academy of Sciences*, *111*(16), 6058. https://doi. org/10.1073/pnas.1317424111

Zhou, Y., Liang, M., Jiang, T., Tian, L., Liu, Y., Liu, Z., ... Kuang, F. (2007). Functional dysconnectivity of the dorsolateral prefrontal cortex in first-episode schizophrenia using resting-state FMRI. *Neuroscience Letters*, *417*(3), 297–302. https://doi.org/10.1016/j.neulet.2007.02.081

Zhou, Y., Shu, N., Liu, Y., Song, M., Hao, Y., Liu, H., ... Jiang, T. (2008). Altered resting-state functional connectivity and anatomical connectivity of hippocampus in schizophrenia. *Schizophrenia Research*, *100*(1–3), 120–132. https://doi.org/10.1016/j.schres.2007.11.039

SUPPORTING INFORMATION

Additional supporting information may be found online in the Supporting Information section at the end of the article.